MULTISCALE MODEL. SIMUL.
Vol. 7, No. 1, pp. 381–406

ON ATOMISTIC-TO-CONTINUUM COUPLING BY BLENDING*

SANTIAGO BADIA†, MICHAEL PARKS‡, PAVEL BOCHEV‡, MAX GUNZBURGER§, AND RICHARD LEHOUCQ‡

Abstract. A mathematical framework for the coupling of atomistic and continuum models by blending them over a subdomain subject to a constraint is developed. Using the framework, four classes of atomistic-to-continuum (AtC) blending methods are established, their consistency is studied, and their relative merits are discussed. In addition, the framework helps clarify the origin of ghost forces and formalizes the notion of a patch test. Numerical experiments with the AtC methods are used to illustrate the theoretical results.

Key words. atomistic-to-continuum coupling, blending methods, multiscale simulation, coupling methods

AMS subject classifications. 65N30, 65N55, 74G15

DOI. 10.1137/07069969X

1. Introduction.

Fully atomistic simulations on an entire model domain are computationally infeasible for many applications of interest. In such cases, a common practice is to replace the atomistic model by a continuum model in all regions where the solution is sufficiently smooth. The two models must then somehow be tied together in an interface region, using a suitable "continuity" condition, or balance principle, for the atomistic and continuum positions or displacements.

Merging of atomistic and continuum models is fundamentally different from merging two continuum models. Because the atomistic model is nonlocal, one cannot simply truncate it to a subregion; care must be taken to compensate for possible surface effects created by missing bonds. Typically, this means that an atomistic-to-continuum (AtC) coupling method cannot rely solely on transmission conditions at a surface. The main focus of this paper is on AtC coupling methods for material statics problems that, in d dimensions, glue the two models over a d-dimensional *blending region* rather than at a $(d-1)$-dimensional manifold.

The roles of a blended model are, first, to provide the correct material response in the blending regions and, second, to couple the two models by enforcing the "con-

*Received by the editors August 8, 2007; accepted for publication (in revised form) January 23, 2008; published electronically April 30, 2008.

http://www.siam.org/journals/mms/7-1/69969.html

†CIMNE, Universitat Politècnica de Catalunya, Jordi Girona 1-3, Edifici C1, 08034 Barcelona, Spain (sbadia@cimne.upc.edu). Current address: Sandia National Laboratories, Computational Mathematics and Algorithms, P.O. Box 5800, MS 1320, Albuquerque, NM 87185. This author's research was supported by the European Community through the Marie Curie contract *NanoSim* (MOIF-CT-2006-039522).

‡Sandia National Laboratories, Computational Mathematics and Algorithms, P.O. Box 5800, MS 1320, Albuquerque, NM 87185 (mlparks@sandia.gov, pbboche@sandia.gov, rblehou@sandia.gov). Sandia is a multiprogram laboratory operated by Sandia Corporation, a Lockheed Martin Company, for the United States Department of Energy's National Nuclear Security Administration under contract DE-AC04-94-AL85000.

§School of Computational Science, Florida State University, Tallahassee, FL 32306-4120 (gunzburg@csit.fsu.edu). This author's research was supported in part by Department of Energy grant DE-FG02-05ER25698.

tinuity" of the atomistic and continuum solutions. Typically, such models are defined using *blending functions* that form a partition of unity in the blending region and *constraint equations* that enforce "continuity" between atomistic and continuum solutions in that region. The constraints may be imposed by either

- using Lagrange multipliers or
- imposing them directly on the degrees of freedom.

The two approaches lead to different AtC operators but are mathematically equivalent. Our analyses exploits this equivalence by relying on the simpler mathematical structure resulting from the second means of enforcing the constraint.

A straightforward way to couple atomistic and continuum models is to superimpose the two models in the blending region. Unfortunately, this *additive* approach leads to unphysical behavior because the resulting energy of the system effectively sums the atomistic and continuum contributions to the energy. To avoid this duplication, the two models must be "blended" together in such a way that the coupled model has the desired physical response. One of our goals will be to state mathematical criteria to quantify such responses by formalizing the notions of patch and consistency tests.

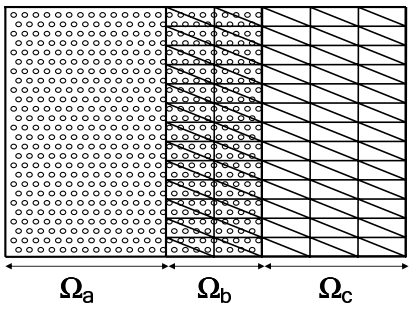

FIG. 1. *The atomistic domain (left), the continuum domain (right), and the blending domain (center).*

The difference between additive and blended couplings can be explained further as follows. Let the problem domain Ω be partitioned into an atomistic region Ω_a, a continuum region Ω_c, and a d-dimensional blending region Ω_b; see Figure 1. Let $\mathcal{L}^a$ and $\mathcal{L}^c$ denote (generally nonlinear) atomistic and continuum operators acting on $\Omega_a \cup \Omega_b$ and $\Omega_b \cup \Omega_c$, respectively.[1] A blending approach to AtC coupling requires the construction of *blended operators* $\mathcal{L}^a_\theta$ and $\mathcal{L}^c_\theta$ defined by a partition of unity in Ω_b and such that $\mathcal{L}^a_\theta = \mathcal{L}^a$ on Ω_a, $\mathcal{L}^c_\theta = \mathcal{L}^c$ on Ω_c. Assume that the atomistic and continuum solutions are connected to each other on Ω_b using a linear constraint operator $\mathcal{C} = (\mathcal{C}_a \ \mathcal{C}_c)$, where $\mathcal{C}_a$ and $\mathcal{C}_c$ act on the atomistic and continuum variables, respectively. Using Lagrange multipliers to enforce the constraint results in the blended AtC operator

$$\begin{pmatrix} \mathcal{L}^a_\theta & 0 & \mathcal{C}^t_a \\ 0 & \mathcal{L}^c_\theta & \mathcal{C}^t_c \\ \mathcal{C}_a & \mathcal{C}_c & 0 \end{pmatrix}.$$

Owing to the definitions of $\mathcal{L}^a_\theta$ and $\mathcal{L}^c_\theta$, no blending occurs outside of Ω_b. In contrast,

[1] In Ω_b, both models apply.

an additive coupling method corresponds to an AtC operator of the form

$$\begin{pmatrix} \mathcal{L}^a & 0 & \mathcal{C}_a^t \\ 0 & \mathcal{L}^c & \mathcal{C}_c^t \\ \mathcal{C}_a & \mathcal{C}_c & 0 \end{pmatrix},$$

in terms of the original atomistic and continuum operators. As a result, the energy in Ω_b is counted twice; this leads to an unphysical response of this coupled AtC model.

AtC coupling via blending is a relatively recent development. In [3], a blending of atomistic and continuum energy functionals was suggested and Lagrange multipliers used for enforcing a set of constraints in the blending domain. The extension to the transient case was considered in [4]. Blending methods for coupling atomistic and continuum equations based on mechanical arguments have recently been proposed in [1, 11]. The Arlequin method introduced in [9] investigated continuum-to-continuum blending. The recent paper [2] presents an analysis of the Arlequin method for a one-dimensional model problem.

The goal of this paper is to develop an abstract framework for AtC coupling methods that can facilitate their formulation and analysis. To provide rigorous criteria for assessing different AtC coupling methods, we also formalize the notions of patch and consistency tests. We are motivated by the increased interest in AtC coupling approaches that is driven by simulation needs in nanotechnology and material sciences. These simulation needs have resulted in the creation of many ad hoc AtC coupling methods that, in many cases, are loosely defined and focused on specific problems. This situation makes the analysis of these methods difficult, even though some efforts have been made in this direction, including analyses of the quasi-continuum method for simple systems [5, 14, 15] and the application of adaptivity and a posteriori error estimation ideas [17].

Using the abstract mathematical framework, we can carry out consistency analyses of AtC blended models. Furthermore, the framework explains the origin of so-called *ghost forces* and the satisfaction of Newton's third law.

The outline of the paper is as follows. Prototype atomistic and continuum models are introduced in section 2. The canonical form of a blended AtC method is stated in section 3. There we also address the issues of consistency and ghost forces. The abstract AtC framework and four classes of AtC methods are presented in section 4. The results of some computational studies are presented in section 5. Concluding remarks are given in section 6.

1.1. Notation. We use blackboard bold fonts ($\mathbb{A}$) for sets of atoms,[2] simple uppercase fonts (A) for atomistic and continuum spaces, calligraphic fonts ($\mathcal{L}$) for operators and functionals, lowercase bold letters ($\boldsymbol{a}$) for vector-valued continuum functions, and lowercase bold Greek letters ($\boldsymbol{\alpha}$) for vector-valued atomistic (discrete) functions and Lagrange multipliers.

Dual spaces are denoted by $(\cdot)'$. In general, discrete and continuous L^2 inner products, L^2 norms, and duality pairings are denoted by $(\cdot,\cdot)$, $\|\cdot\|$, and $\langle\cdot,\cdot\rangle$, respectively. Additional notation will be introduced as needed.

Our convention for designating spaces and affine spaces is as follows: X and Y refer to atomistic and continuum spaces, respectively; a zero subscript, e.g., X_0, indicates that the elements of the space satisfy homogeneous boundary conditions;

[2]The exception to this rule is that $\mathbb{R}^d$ is used to denote d-dimensional Euclidean space and $\mathbb{R} = \mathbb{R}^1$.

the subscript D, e.g., X_D, denotes the (affine) space whose elements satisfy specified inhomogeneous boundary conditions; a lack of subscript, e.g., X, indicates an unconstrained space; a superscript indicates the support of the elements of the space, e.g., X^{ab} denotes that the elements of the space are supported on $\Omega_a \cup \Omega_b$; a lack of superscript, e.g., X, indicates that the elements of the space are supported on all of Ω.

2. The atomistic and continuum models. In this section, we review the atomistic and continuum models that form the basis for the blended AtC coupling models that are the subject of this paper.

2.1. The atomistic model. We consider an undeformed (or reference) lattice $\mathbb{P}$ of identical particles located in a bounded, Euclidean region $\Omega \subset \mathbb{R}^d$. The spatial position vectors of the particle $\alpha \in \mathbb{P}$ in the undeformed and deformed configurations are denoted by $\boldsymbol{x}_\alpha$ and $\boldsymbol{q}_\alpha$, respectively. Thus, the displacement vector of that particle is $\boldsymbol{\psi}_\alpha = \boldsymbol{q}_\alpha - \boldsymbol{x}_\alpha$. The finite-dimensional space of possible atomistic displacements is denoted by X. An element $\boldsymbol{\phi} \in X$ is simply a set of properly ordered[3] $|\mathbb{P}| \times d$ scalar values ϕ_α^i for $\alpha \in \mathbb{P}$ and $i = 1, \ldots, d$.

We denote by $\mathbb{D} \subset \mathbb{P}$ the subset of particles whose positions in the deformed configuration are fixed.[4] We then introduce the affine space of displacements that satisfy the constraints imposed on the particles belonging to $\mathbb{D}$:

$$X_D := \{\boldsymbol{\phi} \in X \ \mid \ \boldsymbol{\phi}_\alpha = \boldsymbol{\psi}_\alpha^{\mathbb{D}} \ \forall\, \alpha \in \mathbb{D}\},$$

where $\boldsymbol{\psi}_\alpha^{\mathbb{D}}$ is the given, fixed displacement vector for the constrained particle $\alpha \in \mathbb{D}$. Similarly, we have the subspace for which the particles belonging to $\mathbb{D}$ have zero displacements:

$$X_0 := \{\boldsymbol{\phi} \in X \ \mid \ \boldsymbol{\phi}_\alpha = \boldsymbol{0} \ \forall\, \alpha \in \mathbb{D}\}.$$

The lattice statics problem consists of finding an equilibrium (deformed) configuration $\{\boldsymbol{\psi}_\alpha\}_{\alpha \in \mathbb{P} \setminus \mathbb{D}}$ that minimizes the potential energy of the particle system, subject to the constraint

$$\boldsymbol{\psi}_\alpha = \boldsymbol{\psi}_\alpha^{\mathbb{D}} \qquad \forall\, \alpha \in \mathbb{D}. \tag{2.1}$$

The minimizer is found by solving the following force-balance problem: given $\boldsymbol{\psi}_\alpha^{\mathbb{D}}$ for all $\alpha \in \mathbb{D}$, find $\boldsymbol{\psi} \in X_D$ such that[5]

$$\big(\mathcal{F}(\boldsymbol{\psi})\big)_\alpha + \boldsymbol{\chi}_\alpha = \boldsymbol{0} \qquad \forall\, \alpha \in \mathbb{P} \setminus \mathbb{D}, \tag{2.2}$$

where $\mathcal{F} : X \to X$ is a (generally nonlinear) operator, $(\mathcal{F}(\cdot))_\alpha$ denotes the internal forces acting on the particle α due to the other particles in $\mathbb{P}$, and $\boldsymbol{\chi}_\alpha$ is the external force applied to the particle α. Note that since $\boldsymbol{\psi} \in X_D$, (2.1) is satisfied. Equation (2.2) is simply Newton's second law for a system of particles interacting via the forces $\mathcal{F}$ and the applied forces $\boldsymbol{\chi}$ and constrained to satisfy (2.1).

A *weak formulation* of (2.2) is given as follows: find $\boldsymbol{\psi} \in X_D$ such that

$$\mathcal{B}^a(\boldsymbol{\psi}, \boldsymbol{\phi}) = \mathcal{G}^a(\boldsymbol{\phi}) \qquad \forall\, \boldsymbol{\phi} \in X_0, \tag{2.3}$$

[3] $|\cdot|$ denotes the cardinality of the set.

[4] In practice, this is a set of particles that are positioned within a layer of the boundary where the displacement is data. This set is the atomistic counterpart of the Dirichlet boundary for a continuum problem.

[5] In general, (2.2) and its weak counterpart (2.3) may not have unique solutions.

where[6]

$$\mathcal{B}^a(\boldsymbol{\psi},\boldsymbol{\phi}) = (\mathcal{F}(\boldsymbol{\psi}),\boldsymbol{\phi}) \quad \text{and} \quad \mathcal{G}^a(\boldsymbol{\phi}) = -(\boldsymbol{\chi},\boldsymbol{\phi}) \quad \text{for } \boldsymbol{\psi} \in X \text{ and } \boldsymbol{\phi} \in X_0. \tag{2.4}$$

Remark 1. Equation (2.3) is the principle of virtual work. Note that the space of test functions is constrained to have vanishing displacements for the particles in $\mathbb{D}$; i.e., the only variations allowed are those for the particles whose positions are not constrained by (2.1). ∎

Remark 2. It is important to note that force balance equations (2.2) are inherently *nonlocal* in nature; i.e., in general, the force acting on a particle $\alpha \in \mathbb{P} \setminus \mathbb{D}$ depends on the displacements of many other particles. ∎

2.2. The continuum model. The spatial position vectors in the undeformed and deformed configurations are denoted by $\boldsymbol{x}$ and $\boldsymbol{q}$, respectively. Thus, the displacement vector is given $\boldsymbol{u} = \boldsymbol{q} - \boldsymbol{x}$. The strong form of the continuum model is given by

$$\mathcal{L}^c\boldsymbol{u} = \boldsymbol{f} \qquad \text{in } \Omega, \tag{2.5a}$$

$$\boldsymbol{u} = \boldsymbol{u}^{\partial\Omega} \qquad \text{on } \partial\Omega, \tag{2.5b}$$

where $\mathcal{L}^c$ denotes a (possibly nonlinear) differential operator, $\boldsymbol{f}$ the external force, $\partial\Omega$ the boundary of Ω, and $\boldsymbol{u}^{\partial\Omega}$ the prescribed boundary data.[7] It is important to note that we assume that the system (2.5) is a *local* model; e.g., the stress at a point $\boldsymbol{x} \in \Omega$ depends on $\boldsymbol{u}$ and $\nabla\boldsymbol{u}$ at that point and not at other points in Ω. This is in contrast to the atomistic model; see Remark 2.

Regarding (2.5) we assume that there exist differential operators[8] $\mathcal{S}(\cdot)$ and $\mathcal{E}(\cdot)$ such that

$$\langle \mathcal{L}^c\boldsymbol{u}, \boldsymbol{v}\rangle = \int_\Omega \mathcal{S}(\boldsymbol{u}) : \mathcal{E}(\boldsymbol{v})\, d\boldsymbol{x}$$

for all smooth functions $\boldsymbol{u}$ and $\boldsymbol{v}$ with $\boldsymbol{v} = \boldsymbol{0}$ on $\partial\Omega$; $(\cdot) : (\cdot)$ denotes the scalar tensor product operation. To state the weak form of (2.5) let Y denote a Hilbert space, defined with respect to Ω, and such that for any $\boldsymbol{v} \in Y$, $\mathcal{S}(\boldsymbol{v})$ and $\mathcal{E}(\boldsymbol{v})$ are meaningful in the L^2 sense. We define the affine subspace and subspace

$$Y_D := \left\{\boldsymbol{v} \in Y \;\middle|\; \boldsymbol{v} = \boldsymbol{u}^{\partial\Omega} \text{ on } \partial\Omega\right\} \qquad \text{and} \qquad Y_0 := \left\{\boldsymbol{v} \in Y \;\middle|\; \boldsymbol{v} = \boldsymbol{0} \text{ on } \partial\Omega\right\},$$

respectively, and the functionals

$$\mathcal{B}^c(\boldsymbol{u},\boldsymbol{v}) := \int_\Omega \mathcal{S}(\boldsymbol{u}) : \mathcal{E}(\boldsymbol{v})\, d\boldsymbol{x} \quad \text{and} \quad \mathcal{G}^c(\boldsymbol{v}) = \langle \boldsymbol{f}, \boldsymbol{v}\rangle \quad \text{for } \boldsymbol{u} \in Y \text{ and } \boldsymbol{v} \in Y_0. \tag{2.6}$$

Then a *weak formulation* of (2.5) is the following: given $\boldsymbol{f} \in (Y_0)'$, find $\boldsymbol{u} \in Y_D$ such that

$$\mathcal{B}^c(\boldsymbol{u},\boldsymbol{v}) = \mathcal{G}^c(\boldsymbol{v}) \qquad \forall\, \boldsymbol{v} \in Y_0. \tag{2.7}$$

Note that, in practice, the operator $\mathcal{E}(\cdot)$ is linear but, in general, $\mathcal{S}(\cdot)$ is nonlinear.

[6] The (generally nonlinear) operator $\mathcal{L}^a$ introduced in section 1 is the operator corresponding to the functional $\mathcal{B}^a(\cdot,\cdot)$; i.e., we have that $\mathcal{L}^a : X \to X'$ satisfies $\mathcal{B}^a(\psi,\phi) = \langle \mathcal{L}^a\psi, \phi\rangle \;\forall\, \phi \in X$. Similar correspondences hold for the other operators $\mathcal{L}^c$, $\mathcal{L}^a_\theta$, and $\mathcal{L}^c_\theta$ introduced in section 1 and the functionals $\mathcal{B}^c(\cdot,\cdot)$, $\mathcal{B}^a_\theta(\cdot,\cdot)$, and $\mathcal{B}^c_\theta(\cdot,\cdot)$, respectively, introduced below.

[7] For simplicity, we consider only Dirichlet boundary conditions.

[8] In general these operators are tensor-valued.

3. Canonical form of blended AtC coupling models. In this section, we propose a canonical structure for blended AtC coupling models for the zero temperature case for which there are no time dependent effects. This structure is the foundation of our abstract blended AtC coupling framework. We also comment on the "ghost force" effect and give formal definitions for consistency and patch tests, thereby providing tools for a rigorous assessment of blended AtC coupling methods.

As mentioned in section 1, the problem domain Ω is partitioned into the nonoverlapping subdomains Ω_a, Ω_b, and Ω_c, as sketched in Figure 1.[9] In particular, Ω_b is in between Ω_a and Ω_c. Let $\mathbb{A}$, $\mathbb{B}$, and $\mathbb{C}$ denote the labels associated with the particles located in Ω_a, Ω_b, and Ω_c, respectively; particles located on the interfaces between Ω_b and the other two subdomains are assigned to $\mathbb{B}$. We assume that

- the atomistic model is valid throughout Ω, i.e., in (2.2), we may choose $\mathbb{P} = \mathbb{A} \cup \mathbb{B} \cup \mathbb{C}$;
- solving (2.2) with $\mathbb{P} = \mathbb{A} \cup \mathbb{B} \cup \mathbb{C}$ for the atomistic displacements is prohibitively expensive; and
- the continuum model (2.5) is valid in Ω_b and Ω_c but not in Ω_a.[10]

The basic principle behind the development of blended AtC coupling models is that one can overcome the high expense associated with using the atomistic model throughout the problem domain Ω by instead employing

- the continuum model in Ω_c where it is valid;
- the atomistic model in Ω_a where the continuum model is not valid;
- a blending[11] of the two models over the region Ω_b that connects the region Ω_a to the region Ω_c.[12]

In the definitions of blended AtC coupling models, we make use of the atomistic subspace and the atomistic affine subspace

$$X_0^{ab} := \{(\boldsymbol{\phi}_\alpha)|_{\alpha\in\mathbb{A}\cup\mathbb{B}} \mid \boldsymbol{\phi} \in X_0\} \qquad \text{and} \qquad X_D^b := \{(\boldsymbol{\phi}_\alpha)|_{\alpha\in\mathbb{B}} \mid \boldsymbol{\phi}_\alpha \in X_D\},$$

respectively. Note that the elements of X_0^{ab} corresponding to the particles located in $\Omega_a \cap \Omega_b$ whose positions are fixed by the boundary conditions vanish, as do those corresponding to all the particles located in Ω_c. The elements of X_D^b corresponding to the particles located in $\Omega_a \cup \Omega_c$ vanish; those corresponding to particles located in Ω_b whose positions are fixed by the boundary condition satisfy the boundary condition (2.1). We will also use the continuum subspace

$$Y_0^{bc} := \{\boldsymbol{v}|_{\Omega_b\cup\Omega_c} \mid \boldsymbol{v} \in Y_0\}$$

and the continuum affine subspaces

$$Y_D^{bc} := \{\boldsymbol{v}|_{\Omega_b\cup\Omega_c} \mid \boldsymbol{v} \in Y_D\} \qquad \text{and} \qquad Y_D^b := \{\boldsymbol{v}|_{\Omega_b} \mid \boldsymbol{v} \in Y_D\}.$$

[9] We do not notationally differentiate between open and closed domains; it should be clear from the specific context which type of domain is being referred to.

[10] If the continuum model is also valid in Ω_a, there would be no need to consider the atomistic model; i.e., one could presumably use the less expensive continuum model (2.7) throughout Ω. On the other hand, if there is not a continuum model that can approximate the atomistic one in *smooth regions* (where the Cauchy–Born hypothesis is valid), AtC algorithms are not suitable.

[11] As was pointed out in section 1, care should be exercised when defining the combined model over the region Ω_b; in particular, one should not simply apply both models there in an additive manner.

[12] An additional implementation principle motivated by efficiency considerations is that the regions Ω_a and Ω_b in which the atomistic model is used should be as small as possible relative to Ω_c, given that one wants to achieve a certain overall accuracy.

Note that the elements of Y_0^{bc} vanish both in Ω_a and on the boundary of $\Omega_b \cap \Omega_c$, while the elements of Y_D^{bc} vanish in Ω_a and satisfy the boundary condition (2.5b) on the boundary segment $(\partial\Omega_b \cup \partial\Omega_c) \cap \partial\Omega$. The elements of Y_D^b vanish in $\Omega_a \cup \Omega_c$; on $\partial\Omega_b \cap \partial\Omega$, they satisfy the boundary condition (2.5b).

In view of the assumptions, principles, and definitions listed above, the *canonical blended AtC coupling model* has the following form: find $\boldsymbol{\psi} \in X_D$ and $\boldsymbol{u} \in Y_D^{bc}$ such that

$$\mathcal{B}_\theta^a(\boldsymbol{\psi}, \boldsymbol{\phi}; \theta_a) + \mathcal{B}_\theta^c(\boldsymbol{u}, \boldsymbol{v}; \theta_c) = \mathcal{G}_\theta^a(\boldsymbol{\phi}; \theta_a) + \mathcal{G}_\theta^c(\boldsymbol{v}; \theta_c) \qquad \forall\, \boldsymbol{\phi} \in X_0^{ab},\, \forall\, \boldsymbol{v} \in Y_0^{bc} \tag{3.1a}$$

$$\text{subject to} \quad \boldsymbol{\psi}_\alpha = \boldsymbol{u}(\boldsymbol{x}_\alpha) \qquad \forall\, \alpha \in \mathbb{C} \setminus (\mathbb{C} \cap \mathbb{D}) \tag{3.1b}$$

$$\text{and} \quad \mathcal{C}(\boldsymbol{\psi}, \boldsymbol{u}) = 0 \quad \text{for} \quad \boldsymbol{\psi} \in X_D^b,\, \boldsymbol{u} \in Y_D^b, \tag{3.1c}$$

where we have

- the *atomistic and continuum blending functions* θ_a and θ_c, respectively, such that $\theta_a \geq 0$, $\theta_c \geq 0$,

$$\theta_a = 1 \text{ in } \Omega_a, \qquad \theta_c = 1 \text{ in } \Omega_c, \qquad \text{and} \qquad \theta_a + \theta_c = 1 \text{ in } \Omega;$$

- the *blended atomistic functionals* $\mathcal{B}_\theta^a(\cdot, \cdot; \theta_a) : X_D \times X_0^{ab} \to \mathbb{R}$ and $\mathcal{G}_\theta^a(\cdot; \theta_a) : X_0^{ab} \to \mathbb{R}$ such that

$$\mathcal{B}_\theta^a(\boldsymbol{\psi}, \boldsymbol{\phi}; 1) = \mathcal{B}^a(\boldsymbol{\psi}, \boldsymbol{\phi}) \quad \text{and} \quad \mathcal{G}_\theta^a(\boldsymbol{\phi}; 1) = \mathcal{G}^a(\boldsymbol{\phi}) \qquad \forall\, \{\boldsymbol{\psi}, \boldsymbol{\phi}\} \in X_D \times X_0^{ab};$$

- the *blended continuous functionals* $\mathcal{B}_\theta^c(\cdot, \cdot; \theta_c) : Y_D^{bc} \times Y_0^{bc} \to \mathbb{R}$ and $\mathcal{G}_\theta^c(\cdot; \theta_c) : Y_0^{bc} \to \mathbb{R}$ such that

$$\mathcal{B}_\theta^c(\boldsymbol{u}, \boldsymbol{v}; 1) = \mathcal{B}^c(\boldsymbol{u}, \boldsymbol{v}) \quad \text{and} \quad \mathcal{G}_\theta^c(\boldsymbol{v}; 1) = \mathcal{G}^c(\boldsymbol{v}) \qquad \forall\, \{\boldsymbol{u}, \boldsymbol{v}\} \in Y_D^{bc} \times Y_0^{bc};$$

- a *constraint operator* $\mathcal{C}(\cdot, \cdot) : X_D^b \times Y_D^b \to Q$, where Q is a function space whose definition depends on the particular nature of the constraints.

Specification of the functionals $\mathcal{B}_\theta^a$, $\mathcal{B}_\theta^c$, $\mathcal{G}_\theta^c$, and $\mathcal{G}_\theta^a$ defines particular blended AtC coupling methods. In section 4, we will define four such methods. The role of the constraint operator $\mathcal{C}(\cdot, \cdot)$ in (3.1c) is to *enforce a suitable notion of continuity between the atomistic and continuum displacements in* Ω_b. In section 3.1, we will discuss some example constraint operators and two ways to enforce this constraint.

The continuum blending function θ_c is required to satisfy the following property.

Assumption 3.1. For every $\boldsymbol{v} \in Y$, we have that $\theta_c \boldsymbol{v} \in Y$.

Remark 3. The elements of the atomistic test function space X_0^{ab} in (3.1a) are supported on $\mathbb{A} \cup \mathbb{B}$ so that the only atomistic force balance (or equilibrium) equations included are those corresponding to the particles located in $\Omega_a \cup \Omega_b$. Analogously, the elements of the continuum test function space Y_0^{bc} are supported on $\Omega_b \cup \Omega_c$ so that continuum contributions from only that domain are included in (3.1a). It is important to note the different causes for the restricted application of these two models. For the atomistic case, we do not include force balance equations for particles located in Ω_c because of *efficiency* reasons; i.e., doing otherwise would make calculations prohibitively expensive. On the other hand, restricting the continuum model to $\Omega_b \cup \Omega_c$ is a matter of *necessity* since it has been assumed that model is not valid in Ω_a. ∎

Remark 4. Clearly, only one blending function need be introduced. Indeed, if we choose a blending function θ such that $0 \leq \theta \leq 1$ throughout Ω, $\theta = 1$ in Ω_a, and $\theta = 0$ on Ω_c, we can then set $\theta_a = \theta$ and $\theta_c = 1 - \theta$. The use of two blending functions θ_a and θ_c instead of just one is purely for notational convenience. Usually, θ is chosen

to be a continuous function. A guiding principle behind its choice over Ω_b is that it be small near the interface between Ω_b and Ω_c (so that θ_a is small there) and that it be close to one near the interface between Ω_a and Ω_b (so that θ_c is small there). Methods for constructing the blending function θ are discussed in [1]. ∎

Remark 5. Only the atomistic force balance equations corresponding to the particles (located) in $\Omega_a \cup \Omega_b$ are included in (3.1a). However, those particles interact with at least some of the particles in Ω_c due to the *nonlocal* nature of the atomistic model. Thus, in general, even if the test function $\boldsymbol{\phi}$ is restricted to the particles in $\Omega_a \cup \Omega_b$, the functional $\mathcal{B}^a_\theta(\cdot,\cdot;\theta_a)$ in (3.1a) includes the displacement of (at least some of) the particles in Ω_c as well as those in $\Omega_a \cup \Omega_b$. For this reason, the atomistic (affine) trial space was chosen to be X_D. Of course, we do not want to solve for the displacements of the particles in Ω_c; indeed, in (3.1a), we have not included the force balance equations corresponding to those particles. Instead, whenever the displacement of a particle in Ω_c is needed in (3.1a), we assume that it is given by the continuum displacement at the location of the particle.[13] This assumption is embodied in (3.1b). ∎

Remark 6. Not properly accounting for the interactions between the particles in $\Omega_a \cup \Omega_b$ and those in Ω_c, e.g., restricting the atomistic *trial* space in (3.1) so that only the particles in $\Omega_a \cup \Omega_b$ are included, results in neglecting the forces acting on the particles in $\Omega_a \cup \Omega_b$ due to the particles in Ω_c. This gives rise to what is known as the *ghost force* effect [13, 16].

The blended AtC coupling model (3.1) mitigates the ghost force effect in two ways. First, as was just discussed, the interactions of particles located in $\Omega_a \cup \Omega_b$ with those in Ω_c are accounted for in (3.1a) and (3.1b). The latter, of course, provides only an approximation to the displacement of the particles located in Ω_c. Any errors introduced through the use of (3.1b) are greatly reduced because the atomistic force balance equations for the particles located in $\Omega_a \cup \Omega_b$ that are near Ω_c involve small values of the blending function Ω_a (see Remark 4) and therefore make small contributions to the overall coupled model.[14] ∎

Remark 7. The continuum model has been assumed to be *local* in nature so that its restriction to $\Omega_b \cup \Omega_c$ does not involve continuum displacements in Ω_a. For this reason, the continuum (affine) trial space was chosen to be Y^{bc}_D.

The ghost force effect that emanates when one neglects the interactions of particles located in $\Omega_a \cup \Omega_b$ with those in Ω_c has been much discussed. Less attention has been paid to the inconsistency that occurs in the continuum model at the interface between Ω_a and Ω_b. Typically, in AtC coupling models, the continuum model (2.5) is not invoked in Ω_a; see Remark 3. It is applied only on $\Omega_b \cup \Omega_c$. Unfortunately, there is no boundary condition available on the interface between $\Omega_b \cup \Omega_c$ and Ω_a that is part of the boundary of the former. Simply restricting the weak form (2.7) of the continuum model to $\Omega_b \cup \Omega_c$ implies the natural boundary condition $\mathcal{S}(\boldsymbol{u}) \cdot \mathbf{n} = \mathbf{0}$ along that interface; in general, this relation is not valid there. Any bad effects due to this discrepancy are greatly mitigated, even eradicated, in blended AtC coupling models of the type (3.1) due to the fact that if θ is chosen to be continuous, then

[13] We are for now interested only in materials where this assumption is valid. In particular, we exclude from Ω_c multilattice materials or materials undergoing phase transitions.

[14] This is clearly the case for atomistic models for which each particle interacts only with other particles that lie within a fixed ball from its position. However, even for the case for which each particle interacts with all other particles, coupled AtC blending models can be defined for which any error in the effects that the particles located in Ω_c have on those located in $\Omega_a \cup \Omega_b$ is greatly reduced due to the blending function θ_a.

$\theta_c = 0$ at the interface in question, and, as a result, $\mathcal{S}(\boldsymbol{u}) \cdot \mathbf{n}$ does not have to equal zero there. ∎

3.1. Defining and enforcing the constraints. The blended AtC coupling system (3.1) involves the constraint equation (3.1c). Before giving some examples of such constraints, we discuss, in general terms, the two ways in which they can be enforced.

The first approach *uses Lagrange multipliers to enforce the constraints* and leads to the *mixed* problem (see, e.g., [7]) given as follows: find $\boldsymbol{\psi} \in X_D$, $\boldsymbol{u} \in Y_D^{bc}$, and $\boldsymbol{\lambda} \in Q'$ such that (3.1b) and

$$\begin{aligned} \mathcal{B}_\theta^a(\boldsymbol{\psi}, \boldsymbol{\phi}; \theta_a) + \mathcal{B}_\theta^c(\boldsymbol{u}, \boldsymbol{v}; \theta_c) + \big\langle \big(l\delta_{\boldsymbol{\psi}}\mathcal{C}(\boldsymbol{\psi}, \boldsymbol{u})\big)\boldsymbol{\phi}, \boldsymbol{\lambda}\big\rangle + \big\langle \big(\delta_{\boldsymbol{u}}\mathcal{C}(\boldsymbol{\psi}, \boldsymbol{u})\big)\boldsymbol{v}, \boldsymbol{\lambda}\big\rangle \\ = \mathcal{G}_\theta^a(\boldsymbol{\phi}; \theta_a) + \mathcal{G}_\theta^c(\boldsymbol{v}; \theta_c) \qquad \forall\, \boldsymbol{\phi} \in X_0^{ab},\ \boldsymbol{v} \in Y_0^{bc}, \end{aligned} \tag{3.2a}$$

$$\langle \mathcal{C}(\boldsymbol{\psi}, \boldsymbol{u}), \boldsymbol{\mu}\rangle = 0 \qquad \forall\, \boldsymbol{\mu} \in Q' \tag{3.2b}$$

are satisfied, where $\delta_{\boldsymbol{\psi}}\mathcal{C}(\cdot,\cdot)$ and $\delta_{\boldsymbol{u}}\mathcal{C}(\cdot,\cdot)$ denote the Gâteaux derivatives of $\mathcal{C}(\cdot,\cdot)$ with respect to $\boldsymbol{\psi}$ and $\boldsymbol{u}$, respectively, and Q' denotes a Lagrange multiplier space whose definition depends on the specific structure of the constraint operator $\mathcal{C}(\cdot,\cdot)$. Since the test functions $\boldsymbol{\phi} \in X_0^{ab}$ and $\boldsymbol{v} \in Y_0^{bc}$ may be chosen independently of each other, (3.2) may be rewritten in the form

$$\mathcal{B}_\theta^a(\boldsymbol{\psi}, \boldsymbol{\phi}; \theta_a) + \big\langle \big(\delta_{\boldsymbol{\psi}}\mathcal{C}(\boldsymbol{\psi}, \boldsymbol{u})\big)\boldsymbol{\phi}, \boldsymbol{\lambda}\big\rangle = \mathcal{G}_\theta^a(\boldsymbol{\phi}; \theta_a) \qquad \forall\, \boldsymbol{\phi} \in X_0^{ab}, \tag{3.3a}$$

$$\mathcal{B}_\theta^c(\boldsymbol{u}, \boldsymbol{v}; \theta_c) + \big\langle \big(\delta_{\boldsymbol{u}}\mathcal{C}(\boldsymbol{\psi}, \boldsymbol{u})\big)\boldsymbol{v}, \boldsymbol{\lambda}\big\rangle = \mathcal{G}_\theta^c(\boldsymbol{v}; \theta_c) \qquad \forall\, \boldsymbol{v} \in Y_0^{bc}, \tag{3.3b}$$

$$\langle \mathcal{C}(\boldsymbol{\psi}, \boldsymbol{u}), \boldsymbol{\mu}\rangle = 0 \qquad \forall\, \boldsymbol{\mu} \in Q'. \tag{3.3c}$$

Note that, in (3.3), coupling between the blended atomistic and continuum models is effected solely through the Lagrange multiplier terms in (3.3a) and (3.3b) and, of course, through the constraint equation (3.3c). Also note that after one discretizes the continuum model and possibly the Lagrange multiplier in (3.3), the result involves not only the atomistic degrees of freedom in $\mathbb{A} \cup \mathbb{B}$ and the continuum degrees of freedom in $\Omega_b \cup \Omega_c$ but also additional Lagrange multiplier degrees of freedom.

The alternate way to enforce the constraint (3.1c) is to *restrict the atomistic and continuum trial affine spaces X_D^b and Y_D^b, respectively, so that their elements satisfy the constraint*. Thus, we define the affine space

$$Z_D^b = \left\{ \boldsymbol{\psi} \in X_D^b,\, \boldsymbol{u} \in Y_D^b \ \middle|\ \mathcal{C}(\boldsymbol{\psi}, \boldsymbol{u}) = 0 \right\}.$$

Correspondingly, we define the subspace of test functions

$$Z_0^b = \left\{ \boldsymbol{\psi} \in X_0^b,\, \boldsymbol{u} \in Y_0^b \ \middle|\ \mathcal{C}(\boldsymbol{\psi}, \boldsymbol{u}) = 0 \right\},$$

where X_0^b and Y_0^b have the obvious definitions. Then (3.1) is equivalent to the following problem: find $\{\boldsymbol{\psi}, \boldsymbol{u}\} \in (X_D^a \times Y_D^c) \oplus (X_D^b \times Y_D^b) \cap Z_D^b$ such that (3.1b) and

$$\begin{aligned} \mathcal{B}_\theta^a(\boldsymbol{\psi}, \boldsymbol{\phi}; \theta_a) + \mathcal{B}_\theta^c(\boldsymbol{u}, \boldsymbol{v}; \theta_c) \\ = \mathcal{G}_\theta^a(\boldsymbol{\phi}; \theta_a) + \mathcal{G}_\theta^c(\boldsymbol{v}; \theta_c) \qquad \forall\, \{\boldsymbol{\phi}, \boldsymbol{v}\} \in (X_0^a \times Y_0^c) \oplus (X_0^b \times Y_0^b) \cap Z_0^b \end{aligned} \tag{3.4}$$

are satisfied. Now coupling between the atomistic and continuum models is effected because the atomistic and continuum test functions $\boldsymbol{\phi}$ and $\boldsymbol{v}$, respectively, cannot be chosen independent of each other but are required to satisfy the constraint. In particular, the division of (3.2a) into (3.3a) and (3.3b) that was effected in the Lagrange

multiplier case is no longer possible. Also note that the number of degrees of freedom in (a discretization of) (3.4) is less than for (3.3). In fact, they are less than the sum of the number of atomistic degrees of freedom in $\mathbb{A} \cup \mathbb{B}$ and the continuum degrees of freedom in $\Omega_b \cup \Omega_c$.

Remark 8. It is important to note that the two approaches for the enforcement of constraints are equivalent in the sense that the solutions obtained using either approach are identical. □

If a basis for Z_0 is easy to construct, then the second approach is more appealing since it involves fewer degrees of freedom. It is also more convenient for theoretical analyses[15] of AtC coupling methods because it does not require the consideration of an additional inf-sup compatibility condition between the Lagrange multiplier space and the atomistic and continuum spaces.

3.1.1. Example constraints. We briefly consider examples for the operator $\mathcal{C}$ appearing in (3.1). While this operator can have a rather general form, here we focus primarily on definitions of linear constraint operators. Thus, we consider constraints of the type

$$\mathcal{C}_a(\boldsymbol{\psi}) - \mathcal{C}_c(\boldsymbol{u}) = 0 \qquad \text{for} \quad \boldsymbol{\psi} \in X_D^b,\, \boldsymbol{u} \in Y_D^b,$$

where $\mathcal{C}_a(\cdot) : X_D^b \to Q$ and $\mathcal{C}_c(\cdot) : Y_D^b \to Q$ are linear operators.

A choice that allows for the elimination of all atomistic degrees of freedom in Ω_b from blended AtC coupling models is given by

$$\boldsymbol{\psi}_\alpha = \boldsymbol{u}(\boldsymbol{x}_\alpha) \qquad \forall\, \alpha \in \mathbb{B} \setminus (\mathbb{B} \cap \mathbb{D}) \tag{3.5}$$

so that $Q = X_D^b$. The particle displacements of the particles in Ω_b are slaved to the continuum displacements.[16] Thus, the displacements of the particles in Ω_b can easily be eliminated from the set of degrees of freedom.[17] The physical assumption embodied in (3.5) is that the continuous (macroscopic) and atomistic (microscopic) deformation fields should agree. This is precisely the case for a Cauchy–Born deformation [6, 10].

Equation (3.5) is the "extreme" case of constraint equations of the type

$$\boldsymbol{\psi} = \Pi_{\mathbb{B}}(\boldsymbol{u}), \tag{3.6}$$

where $\Pi_{\mathbb{B}} : Y_D^b \mapsto X_D^b$ is an *expansion* operator; in this case we have that $Q = X_D^b$. Again, we say that, in Ω_b, *the particle displacements are slaved to the continuous displacement field* but perhaps in a more complex manner than that for (3.5). As a result, the degrees of freedom that determine the particle displacements in Ω_b can easily be eliminated.

In principle, one can instead define constraint operators of the type

$$\boldsymbol{u} = \pi_b(\boldsymbol{\psi}), \tag{3.7}$$

where now $\pi_b : X_D^b \mapsto Y_D^b$ is a *compression* operator and $Q = Y_D^b$. Now, in Ω_b, *the continuous displacement field is slaved to the particle displacements.* As a result,

[15] Since (3.3) and (3.4) are equivalent (see Remark 8), their properties can be studied using either one of them.

[16] In fact, they are slaved in exactly the same way as in (3.1b) for the particles in Ω_c.

[17] In [3], a nonlinear version of (3.5) is used. Specifically, there it is required that $|\boldsymbol{\psi}_\alpha - \boldsymbol{u}(\boldsymbol{x}_\alpha)| = 0$ $\forall\, \alpha \in \mathbb{B} \setminus (\mathbb{B} \cap \mathbb{D})$, where $|\cdot|$ denotes the Euclidean norm in $\mathbb{R}^d$. Clearly, this constraint and the linear, vectorial version (3.5) are the same. The nonlinear version requires fewer Lagrange multipliers (one instead of d per particle) than does the linear version (3.5). On the other hand, for the linear version, it is much easier to implement restrictions of the test and trial spaces that satisfy the constraint.

the degrees of freedom that determine, e.g., the finite element approximation of the continuous displacement in Ω_b can easily be eliminated.

Remark 9. It is important to note that the use of, e.g., (3.5) to eliminate the atomistic degrees of freedom in Ω_b does not imply that the atomistic force balance equations in the blending region Ω_b are deleted from the blended AtC coupling model (3.1), as is done in the quasi-continuum method [18]. What it does mean is that the atomistic test function $\boldsymbol{\phi}$ is constrained to satisfy $\boldsymbol{\phi}_\alpha = \boldsymbol{v}(\boldsymbol{x}_\alpha)$ for all $\alpha \in \mathbb{B} \setminus (\mathbb{B} \cap \mathbb{D})$, where $\boldsymbol{v}$ denotes the continuum test function. Thus, from (3.4), we have, for test functions supported in Ω_b, that (3.1a) reduces to a linear combination of the atomistic and continuum models. ∎

For constraints of the type (3.6) or (3.7), one of the operators $\mathcal{C}_a$ and $\mathcal{C}_c$ is the identity operator; as a result, either the atomistic or continuum degrees of freedom can easily be eliminated. One can also define constraint equations for which neither of these operators is so simple. Two such examples use a subdivision $\{\Omega_{b,j}\}_{j=1}^J$ of Ω_b into J nonoverlapping, covering subdomains; i.e., $\Omega_{b,j} \cap \Omega_{b,k} = \emptyset$ whenever $j \neq k$ and $\cup_{j=1}^J \Omega_{b,j} = \Omega_b$. We denote the volume of $\Omega_{b,j}$ by $|\Omega_{b,j}|$. This subdivision of Ω_b engenders the subdivision of $\{\mathbb{B}_j\}_{j=1}^J$ of $\mathbb{B}$, where $\alpha \in \mathbb{B}_j$ whenever $\boldsymbol{x}_\alpha \in \Omega_{b,j}$. We denote the number of particles located in $\Omega_{b,j}$ by $|\mathbb{B}_j|$. A constraint set that is less stringent than (3.5) is then given by

$$\frac{1}{|\Omega_{b,j}|} \int_{\Omega_{b,j}} \boldsymbol{u}\, d\boldsymbol{x} = \frac{1}{|\mathbb{B}_j|} \sum_{\alpha \in \mathbb{B}_j} \boldsymbol{\psi}_\alpha \qquad \text{for } j = 1, \ldots, J.$$

If one approximates the integral in the left-hand side by a simple average, one obtains the constraint equations

$$\sum_{\alpha \in \mathbb{B}_j} \boldsymbol{u}(\boldsymbol{x}_\alpha) = \sum_{\alpha \in \mathbb{B}_j} \boldsymbol{\psi}_\alpha \qquad \text{for } j = 1, \ldots, J. \tag{3.8}$$

In either case, we have that $Q = \mathbb{R}^{Jd}$.

Comparing (3.5) and (3.8), we note that while the former relation slaves every atomistic displacement to the continuum displacement field, the latter relates averages of the atomistic displacement to averages of the continuum displacements. Constraints such as (3.8) that involve linear combinations of displacement values are difficult to enforce through restrictions of the test and trial spaces so that the Lagrange multiplier approach is more useful in this case.[18] For the constraint equations (3.8), one defines the Lagrange multipliers to be piecewise constant functions with respect to the subdivision $\{\Omega_{b,j}\}_{j=1}^J$ of Ω_b.

3.2. AtC consistency and the patch test. This section introduces a well-defined notion of AtC *consistency* and a patch test that can be used to evaluate AtC coupled models.

Definition 3.1 (consistency test problem). *The set* $\{\boldsymbol{\chi}, \boldsymbol{\psi}^{\mathbb{D}}; \boldsymbol{f}, \boldsymbol{u}^{\partial\Omega}\}$ *is called a* consistency test problem *if the solutions* $\widetilde{\boldsymbol{\psi}}$ *and* $\widetilde{\boldsymbol{u}}$ *of the global problems* (2.3) *and* (2.7)*, respectively,*[19] *are such that* $\mathcal{C}(\widetilde{\boldsymbol{\psi}}, \widetilde{\boldsymbol{u}}) = 0$ *holds on* Ω.

Definition 3.2 (patch test problem). *A consistency test problem is called a* patch test problem *if the continuous component* $\widetilde{\boldsymbol{u}}$ *of* $(\widetilde{\boldsymbol{\psi}}, \widetilde{\boldsymbol{u}})$ *is such that* $\mathcal{S}(\widetilde{\boldsymbol{u}})$ *is constant; i.e.,* $\widetilde{\boldsymbol{u}}$ *is a constant stress solution.*

[18] For constraints of the type (3.6) or (3.7), including the special case (3.5), restricting the test and trial spaces is easily accomplished.

[19] Recall that $\{\boldsymbol{\chi}, \boldsymbol{\psi}^{\mathbb{D}}; \boldsymbol{f}, \boldsymbol{u}^{\partial\Omega}\}$ provides the data for these two problems.

The following definitions formalize the notion of *passing a patch test* and a definition of *consistency* for an AtC coupling method.

DEFINITION 3.3 (passing a patch test problem). *Assume that* $\{\boldsymbol{\chi}, \boldsymbol{\psi}^{\mathbb{D}}; \boldsymbol{f}, \boldsymbol{u}^{\partial\Omega}\}$ *is a patch test problem with solution* $(\widetilde{\boldsymbol{\psi}}, \widetilde{\boldsymbol{u}})$. *An* AtC coupling method passes a patch test *if* $(\widetilde{\boldsymbol{\psi}}, \widetilde{\boldsymbol{u}})$ *satisfies the AtC coupled problem* (3.3) *or* (3.4).

DEFINITION 3.4 (AtC consistency). *An AtC coupling method is* consistent *if, for any consistency test problem, the pair* $(\widetilde{\boldsymbol{\psi}}, \widetilde{\boldsymbol{u}})$ *satisfies the coupled AtC system.*

Atomistic problems with Cauchy–Born solutions (see [6, 10]) are a physical example of consistency test problems. From the previous definitions, one can easily infer that consistency implies passage of the patch test problem. However, the converse statement is not true.

4. Blended AtC coupling methods. In this section, we establish four general paths for defining how the blended functionals $\mathcal{B}^c_\theta$, $\mathcal{B}^a_\theta$, $\mathcal{G}^c_\theta$, and $\mathcal{G}^a_\theta$ appearing in (3.1) are obtained from the original atomistic and continuum functionals (2.4) and (2.6), respectively. Then we determine whether the four resulting classes of blended AtC coupling methods are consistent and pass the patch test of section 3.2.

We consider two different ways of defining both the atomistic and continuum blended functionals $\mathcal{B}^a_\theta(\boldsymbol{\psi}, \boldsymbol{\phi}; \theta_a)$ and $\mathcal{B}^c_\theta(\boldsymbol{u}, \boldsymbol{v}; \theta_c)$. The first way is to directly use their respective unblended counterparts $\mathcal{B}^a(\boldsymbol{\psi}, \boldsymbol{\phi})$ and $\mathcal{B}^c(\boldsymbol{u}, \boldsymbol{v})$ defined in (2.4) and (2.6), respectively. We refer to this approach as *external* blending because the definitions of the original atomistic and continuum functionals do not change. The second possibility is to define the blended operators and functionals by carefully changing their internal definitions. We refer to this approach as *internal* blending because it requires changes to the definition of the atomistic and continuum functionals.

The specific choices we make are as follows. For the atomistic blended functional, we have the choices

$$\mathcal{B}^a_\theta(\boldsymbol{\psi}, \boldsymbol{\phi}; \theta_a) = \begin{cases} \mathcal{B}^a(\boldsymbol{\psi}, \boldsymbol{\Theta_a}\boldsymbol{\phi}) = (\mathcal{F}(\boldsymbol{\psi}), \boldsymbol{\Theta_a}\boldsymbol{\phi}) & \Longleftarrow \text{external} \\ \quad \text{or} & \\ \big(\mathcal{F}_\theta(\boldsymbol{\psi}; \theta_a), \boldsymbol{\phi}\big) & \Longleftarrow \text{internal} \end{cases} \tag{4.1}$$

for all $\boldsymbol{\psi} \in X_D$ and $\boldsymbol{\phi} \in X_0^{ab}$, where $\boldsymbol{\Theta_a}$ is a diagonal weighting matrix whose diagonal values are equal to θ_a evaluated at the corresponding particle positions:

$$(\boldsymbol{\Theta_a})^{ij}_{\alpha\beta} = \delta_{ij}\delta_{\alpha\beta}\theta_a(\boldsymbol{x}_\alpha) \qquad \text{for } i, j = 1, \ldots, d,\ \alpha, \beta \in \mathbb{P}.$$

A discussion about how $\mathcal{F}_\theta(\boldsymbol{\psi}; \theta_a)$ may be defined is given in section 5; further details are given in [1].

For the continuum blended functional, we have the choices

$$\mathcal{B}^c_\theta(\boldsymbol{u}, \boldsymbol{v}; \theta_c) = \begin{cases} \mathcal{B}^c(\boldsymbol{u}, \theta_c\boldsymbol{v}) = \displaystyle\int_{\Omega_b \cup \Omega_c} \mathcal{S}(\boldsymbol{u}) : \mathcal{E}(\theta_c\boldsymbol{v})\, d\boldsymbol{x} & \Longleftarrow \text{external} \\ \quad \text{or} & \\ \displaystyle\int_{\Omega_b \cup \Omega_c} \theta_c \mathcal{S}(\boldsymbol{u}) : \mathcal{E}(\boldsymbol{v})\, d\boldsymbol{x} & \Longleftarrow \text{internal} \end{cases} \tag{4.2}$$

for all $\boldsymbol{u} \in Y_D^{bc}$ and $\boldsymbol{v} \in Y_0^{bc}$.

For either choice made in (4.1) and (4.2), the blended linear data functionals appearing in (3.1) are defined as

$$\mathcal{G}^a_\theta(\boldsymbol{\phi}; \theta_a) = \mathcal{G}^a(\Theta_a\boldsymbol{\phi}) = -(\boldsymbol{\chi}, \boldsymbol{\Theta_a}\boldsymbol{\phi}) = -(\boldsymbol{\Theta_a}\boldsymbol{\chi}, \boldsymbol{\phi}) \qquad \forall\, \boldsymbol{\phi} \in X_0^{ab} \tag{4.3}$$

and

$$\mathcal{G}^c_\theta(\boldsymbol{v};\theta_c) = \mathcal{G}^c(\theta_c\boldsymbol{v}) = \langle \boldsymbol{f}, \theta_c\boldsymbol{v}\rangle = \langle \theta_c\boldsymbol{f}, \boldsymbol{v}\rangle = \int_{\Omega_b\cup\Omega_c} \theta_c\boldsymbol{f}\cdot\boldsymbol{v}\,d\boldsymbol{x} \qquad \forall\,\boldsymbol{v}\in Y_0^{bc}, \tag{4.4}$$

respectively. Note that we can restrict the integrals in (4.2) and (4.4) to $\Omega_b\cup\Omega_c$ by virtue of the fact that, by the definition of the test space Y_0^{bc}, the continuum test function $\boldsymbol{v}$ is supported only within that subregion.

Because external and internal blending can be applied independently to the continuum and atomistic problems, it follows that we have a total of four possible choices for the combined blending functional $\mathcal{B}^a(\boldsymbol{\psi},\boldsymbol{\phi};\theta_a) + \mathcal{B}^c_\theta(\boldsymbol{u},\boldsymbol{v};\theta_c)$ appearing in (3.1). The four choices are summarized in Table 4.1.

TABLE 4.1
Blended AtC coupling methods classified by blending types.

Method	Blending approach	
	Atomistic	Continuum
I	external	internal
II	internal	internal
III	external	external
IV	internal	external

In the next four sections, we discuss blended AtC coupling methods belonging to each one the four classes and investigate their properties.

4.1. Method I. In this method, we use external atomistic blending and internal continuum blending. Thus, (3.1) is given by the following: find $\boldsymbol{\psi}\in X_D$ and $\boldsymbol{u}\in Y_D^{bc}$ such that (3.1b), (3.1c), and

$$\begin{aligned}\big(\mathcal{F}(\boldsymbol{\psi}),\boldsymbol{\Theta_a}\boldsymbol{\phi}\big) + \int_{\Omega_b\cup\Omega_c}\theta_c\mathcal{S}(\boldsymbol{u}):\mathcal{E}(\boldsymbol{v})\,d\boldsymbol{x}&\\ = -\left(\boldsymbol{\chi},\boldsymbol{\Theta_a}\boldsymbol{\phi}\right) + \int_{\Omega_b\cup\Omega_c}\theta_c\boldsymbol{f}\cdot\boldsymbol{v}\,d\boldsymbol{x} \qquad \forall\,\boldsymbol{\phi}\in X_0^{ab},\ \boldsymbol{v}\in Y_0^{bc}&\end{aligned} \tag{4.5}$$

are satisfied. For this method, we have the following result.

THEOREM 4.1. *Method* I *defined by* (4.5) *is not consistent and does not pass the patch test.*

Proof. Let $\{\widetilde{\boldsymbol{\psi}},\widetilde{\boldsymbol{u}}\}$ be a solution of the consistency test problem defined in section 3.2. Clearly, $\boldsymbol{\Theta_a}\boldsymbol{\phi}\in X_0^{ab}\subset X_0$ whenever $\boldsymbol{\phi}\in X_0^{ab}$ so that, from (2.3), we have that

$$\big(\mathcal{F}(\widetilde{\boldsymbol{\psi}}),\boldsymbol{\Theta_a}\boldsymbol{\phi}\big) + \left(\boldsymbol{\chi},\boldsymbol{\Theta_a}\boldsymbol{\phi}\right) = 0 \qquad \forall\,\boldsymbol{\phi}\in X_0^{ab} \tag{4.6}$$

so that the atomistic terms in (4.5) cancel.

From Assumption 3.1, we have that, for sufficiently smooth θ_c, $\theta_c\boldsymbol{v}\in Y_0^{bc}\subset Y_0$ whenever $\boldsymbol{v}\in Y_0^{bc}$. Then, from (2.7) and since $\mathcal{E}(\cdot)$ is a linear operator, we have that

$$\int_{\Omega_b\cup\Omega_c}\theta_c\mathcal{S}(\widetilde{\boldsymbol{u}}):\mathcal{E}(\boldsymbol{v})\,d\boldsymbol{x} - \int_{\Omega_b\cup\Omega_c}\theta_c\boldsymbol{f}\cdot\boldsymbol{v}\,d\boldsymbol{x} = -\int_{\Omega_b\cup\Omega_c}\boldsymbol{v}\cdot\mathcal{S}(\widetilde{\boldsymbol{u}})\cdot\mathcal{E}(\theta_c)\,d\boldsymbol{x}$$

so that the continuum terms in (4.5) cancel if and only if

$$\mathcal{S}(\widetilde{\boldsymbol{u}})\cdot\mathcal{E}(\theta_c) = \boldsymbol{0} \qquad \text{almost everywhere in } \Omega_b\cup\Omega_c. \tag{4.7}$$

This relation is, in general, not true in Ω_b. In particular, for a patch test problem, (4.7) is true only if $\mathcal{E}(\theta_c) = 0$ in $\Omega_b \cup \Omega_c$, which in practice implies that θ_c must be constant.[20] ∎

Remark 10. Let us consider discretization of the continuum terms in (4.5) using the finite element space $Y^h \subset Y^h$, the subspace $Y_0^h \subset Y_0$, and the affine subspace $Y_D^h \subset Y^h$ along with a piecewise smooth approximation θ_c^h of the blending function θ_c, defined with respect to the same mesh. Then we have the following discretized problem: find $\boldsymbol{\psi}_h \in X_D$ and $\boldsymbol{u}_h \in Y_D^{h,bc}$ such that

$$\begin{aligned}(\mathcal{F}(\boldsymbol{\psi}_h), \boldsymbol{\Theta_a}\boldsymbol{\phi}) + \int_{\Omega_b\cup\Omega_c} \theta_c^h \mathcal{S}(\boldsymbol{u}_h) : \mathcal{E}(\boldsymbol{v})\, d\boldsymbol{x} \\ = (\boldsymbol{\chi}, \boldsymbol{\Theta_a}\boldsymbol{\phi}) + \int_{\Omega_b\cup\Omega_c} \theta_c^h \boldsymbol{f}\cdot\boldsymbol{v}\, d\boldsymbol{x} \qquad \forall\, \boldsymbol{\phi} \in X_0^{ab},\ \boldsymbol{v} \in Y_0^{h,bc}\end{aligned} \tag{4.8}$$

is satisfied along with suitable discretizations of (3.1b) and (3.1c).

Note that, in general, $\theta_c^h \boldsymbol{v}_h \notin Y_0^{h,bc}$ so that Assumption 3.1 applied to the discrete spaces does not hold. As a result, Theorem 4.1 cannot be used to assert whether or not (4.8) passes the patch test. However, the proof of that theorem can easily be adapted to the discretized case. Given a consistency test solution $\{\widetilde{\boldsymbol{\psi}}_h, \widetilde{\boldsymbol{u}}_h\}$, it is easy to see that the atomistic terms in (4.8) again cancel. The finite element approximation $\widetilde{\boldsymbol{u}}_h$ of the solution of (2.7) satisfies

$$\int_{\Omega_b\cup\Omega_c} \mathcal{S}(\widetilde{\boldsymbol{u}}_h) : \mathcal{E}(\boldsymbol{v})\, d\boldsymbol{x} = \int_{\Omega_b\cup\Omega_c} \boldsymbol{f}\cdot\boldsymbol{v}\, d\boldsymbol{x} \qquad \forall\, \boldsymbol{v} \in Y_0^{h,bc}$$

so that, in general, the continuum terms in (4.8) do not cancel. Even if we were to choose θ_c^h to be a piecewise constant function with respect to the finite element mesh in Ω_b, the consistency condition would require that

$$\sum_e \int_{\Omega_e} \theta_c^h \mathcal{S}(\widetilde{\boldsymbol{u}}_h) : \mathcal{E}(\boldsymbol{v})\, d\boldsymbol{x} = \sum_e \int_{\Omega_e} \theta_c^h \boldsymbol{f}\cdot\boldsymbol{v}\, d\boldsymbol{x},$$

where $\sum_e$ denotes a sum over the finite elements. If θ_c^h is piecewise constant, this condition can hold only if

$$\int_{\Omega_e} \mathcal{S}(\widetilde{\boldsymbol{u}}_h) : \mathcal{E}(\boldsymbol{v})\, d\boldsymbol{x} = \int_{\Omega_e} \boldsymbol{f}\widetilde{\boldsymbol{v}}_h\, d\boldsymbol{x}$$

with respect to every finite element Ω_e. This is not true in general. ∎

4.2. Method II. The reason Method I fails to be consistent is that for a solution of the consistency test problem, the atomistic terms in (4.5) vanish, but the continuum terms do not. For Method II, we modify the atomistic terms in the hope that, for such solutions, they can "cancel" out the continuum terms. To this end, we use internal atomistic and continuum blending. Thus, (3.1) is given by the following: find $\boldsymbol{\psi} \in X_D$ and $\boldsymbol{u} \in Y_D^{bc}$ such that (3.1b), (3.1c), and

$$\begin{aligned}\big(\mathcal{F}_\theta(\boldsymbol{\psi};\theta_a), \boldsymbol{\phi}\big) + \int_{\Omega_b\cup\Omega_c} \theta_c \mathcal{S}(\boldsymbol{u}) : \mathcal{E}(\boldsymbol{v})\, d\boldsymbol{x} \\ = -(\boldsymbol{\chi}, \boldsymbol{\Theta_a}\boldsymbol{\phi}) + \int_{\Omega_b\cup\Omega_c} \theta_c \boldsymbol{f}\cdot\boldsymbol{v}\, d\boldsymbol{x} \qquad \forall\, \boldsymbol{\phi} \in X_0^{ab},\ \boldsymbol{v} \in Y_0^{bc}\end{aligned} \tag{4.9}$$

[20] In the case of linear elasticity, (4.7) corresponds to $\nabla\widetilde{\boldsymbol{u}}\cdot\nabla\theta_c = \boldsymbol{0}$ almost everywhere in $\Omega_b \cup \Omega_c$. As a result, Method I will pass a patch test if and only if $\nabla\theta_c = \boldsymbol{0}$ in $\Omega_b \cup \Omega_c$. Since, by definition, $\theta_c = 1$ in Ω_c and $\theta_c = 0$ in Ω_a, this relation is impossible to satisfy with θ_c continuous in Ω.

are satisfied.

The consistency of this method depends on the definition of the operator $\mathcal{F}_\theta(\cdot;\theta_a)$. The following theorem gives an abstract consistency condition for this operator.

THEOREM 4.2. *Under Assumption* 3.1*, Method* II *is consistent if the operator* $\mathcal{F}_\theta(\cdot;\theta_a)$ *is constructed in such a way that any consistency test problem solution* $\{\widetilde{\boldsymbol{\psi}},\widetilde{\boldsymbol{u}}\}$ *satisfies*

$$\big(\mathcal{F}_\theta(\widetilde{\boldsymbol{\psi}};\theta_a),\boldsymbol{\phi}\big)-\big(\mathcal{F}(\widetilde{\boldsymbol{\psi}}),\boldsymbol{\Theta}_a\boldsymbol{\phi}\big)=-\int_{\Omega_b\cup\Omega_c}\Big(\theta_c\mathcal{S}(\widetilde{\boldsymbol{u}}):\mathcal{E}(\boldsymbol{v})-\mathcal{S}(\widetilde{\boldsymbol{u}}):\mathcal{E}(\theta_c\boldsymbol{v})\Big)\,d\boldsymbol{x} \tag{4.10}$$

for all $\boldsymbol{\phi}\in X_0^{ab}$ *and* $\boldsymbol{v}\in Y_0^{bc}$*. Method* II *passes the patch test if* (4.10) *is satisfied for patch test solutions.*

Proof. We have that $\boldsymbol{\Theta}_a\boldsymbol{\phi}\in X_0^{ab}$ whenever $\boldsymbol{\phi}\in X_0^{ab}$ and, by Assumption 3.1, that $\theta_c\boldsymbol{v}\in Y_0^{bc}$ whenever $\boldsymbol{v}\in Y_0^{bc}$. Then, by definition, a consistency test problem solution $\{\widetilde{\boldsymbol{\psi}},\widetilde{\boldsymbol{u}}\}$ satisfies

$$\big(\mathcal{F}(\widetilde{\boldsymbol{\psi}}),\boldsymbol{\Theta}_a\boldsymbol{\phi}\big)=-\left(\boldsymbol{\chi},\Theta_a\boldsymbol{\phi}\right)\qquad\forall\,\boldsymbol{\phi}\in X_0^{ab}\subset X_0$$

and

$$\int_{\Omega_b\cup\Omega_c}\mathcal{S}(\widetilde{\boldsymbol{u}}):\mathcal{E}(\theta_c\boldsymbol{v})\,d\boldsymbol{x}=\int_{\Omega_b\cup\Omega_c}\theta_c\boldsymbol{f}\cdot\boldsymbol{v}\,d\boldsymbol{x}\qquad\forall\,\boldsymbol{v}\in Y_0^{bc}\subset Y_0. \tag{4.11}$$

Using the last two equations, it is easily seen that a consistency test problem solution $\{\widetilde{\boldsymbol{\psi}},\widetilde{\boldsymbol{u}}\}$ satisfies (4.9) only if (4.10) holds. ∎

In [1], a specific choice for $\mathcal{F}_\theta(\cdot;\theta_a)$ is defined that satisfies (4.10) for a particular set of one-dimensional patch test problems. The choice can be mechanically justified as a *blended force balance*. In section 5, we show through numerical experimentation that the method suggested there is much more accurate than Method I. Furthermore, among the four methods we discuss here, *Method* II *is the only method that leads to a symmetric AtC coupling operator.*[21] This feature of Method II has a positive effect on its stability properties and results in symmetric linear systems that are easier to solve than the nonsymmetric linear systems generated by the other three methods.

4.3. Method III. One of the assumptions used for the design of AtC coupling algorithms is that the continuum model is a good approximation of the atomistic model in Ω_b and Ω_c. This assumption implies that the continuum differential operator $\mathcal{L}$ is a good representation of $\mathcal{F}$ under suitable conditions, e.g., smoothness. Thus, a seemingly reasonable approach would be to blend the operators $\mathcal{L}$ and $\mathcal{F}$. This approach leads to the following blended AtC coupling method that uses external atomistic and continuum blending: find $\boldsymbol{\psi}\in X_D$ and $\boldsymbol{u}\in Y_D^{bc}$ such that (3.1b), (3.1c), and

$$\begin{aligned}\big(\mathcal{F}(\psi),\boldsymbol{\Theta}_a\boldsymbol{\phi}\big)+\int_{\Omega_b\cup\Omega_c}\mathcal{S}(\boldsymbol{u}):\mathcal{E}(\theta_c\boldsymbol{v})\,d\boldsymbol{x}\\ =-\left(\boldsymbol{\chi},\boldsymbol{\Theta}_{\boldsymbol{a}}\boldsymbol{\phi}\right)+\int_{\Omega_b\cup\Omega_c}\theta_c\boldsymbol{f}\cdot\boldsymbol{v}\,d\boldsymbol{x}\qquad\forall\,\boldsymbol{\phi}\in X_0^{ab},\,\boldsymbol{v}\in Y_0^{bc}\end{aligned} \tag{4.12}$$

are satisfied.[22]

[21] Of course, this is possible only when both the atomistic and continuum models are symmetric to start with.

[22] This method can be understood as a *residual blending method* since it blends $\mathcal{L}\boldsymbol{u}-\boldsymbol{f}$ and $\mathcal{F}(\psi)-\boldsymbol{\chi}$.

A positive feature of this approach that is not shared by the other three methods is that for a consistency problem solution, the atomistic and continuum terms in (4.9) separately cancel out; see (4.6) and (4.11). The following theorem is a direct consequence of this observation.

THEOREM 4.3. *Under Assumption* 3.1*, Method* III *is consistent and therefore passes the patch test.*

4.4. Method IV. The fourth method can be viewed as a "dual" of Method I in that it uses internal atomistic blending and external continuum blending. It is defined as follows: find $\boldsymbol{\psi} \in X_D$ and $\boldsymbol{u} \in Y_D^{bc}$ such that (3.1b), (3.1c), and

$$\begin{aligned} \big(\mathcal{F}_\theta(\boldsymbol{\psi};\theta_a),\boldsymbol{\phi}\big) + \int_{\Omega_b\cup\Omega_c} \theta_c \mathcal{S}(\boldsymbol{u}) : \mathcal{E}(\boldsymbol{v})\, d\boldsymbol{x} \\ = -\left(\boldsymbol{\chi}, \boldsymbol{\Theta_a}\boldsymbol{\phi}\right) + \int_{\Omega_b\cup\Omega_c} \theta_c \boldsymbol{f}\cdot\boldsymbol{v}\, d\boldsymbol{x} \qquad \forall\, \boldsymbol{\phi}\in X_0^{ab},\ \boldsymbol{v}\in Y_0^{bc} \end{aligned} \tag{4.13}$$

are satisfied. In this case, the continuous terms cancel for any consistency problem solution, but the atomistic terms do not. As a result, this method is not consistent, and so it does not pass the patch test.

4.5. Summary and comparison of the four methods. We summarize and compare the consistency of the four different methods in Table 4.2.

TABLE 4.2
Values of the atomistic and continuous contributions to the blended AtC coupling methods evaluated at a consistency problem solution $\{\widetilde{\boldsymbol{\psi}},\widetilde{\boldsymbol{u}}\}$.

Method	$\mathcal{B}_\theta^a(\widetilde{\boldsymbol{\psi}},\boldsymbol{\phi}) - \mathcal{G}_\theta^a(\boldsymbol{\phi})$	$\mathcal{B}_\theta^c(\widetilde{\boldsymbol{u}},\boldsymbol{v}) - \mathcal{G}_\theta^c(\boldsymbol{v})$	Is it consistent?
I	$=0$	$\neq 0$	No
II	$\neq 0$	$\neq 0$	Depends on $\mathcal{F}_{\theta_a}$
III	$=0$	$=0$	Yes
IV	$\neq 0$	$=0$	No

At least two of the methods we have introduced have appeared previously. What we refer to as Method I was described in [3]; see equations (10) and (11) of that paper; Method II was introduced in [1, 11]. We also remark that Methods I, III, and IV do not satisfy Newton's third law over the blend region, and so these methods do not lead to a symmetric formulation.

We also contrast AtC blending with the quasi-continuum method [18]. In a local quasi-continuum method, the Cauchy–Born hypothesis [6] is used to eliminate degrees of freedom in a particle model, lessening the computational complexity. The local quasi-continuum approximation has no direct relation to blending. In certain circumstances, the local/nonlocal interface arising in the quasi-continuum method can be viewed as the blending approach of Method II with a $(d-1)$-dimensional interface; see [8]. Furthermore, the forces in the quasi-continuum method are derived from a global energy functional and obey Newton's third law (or, equivalently, the conservation of linear momentum).

5. Numerical results. In this section, we report on the results of some simple computations for one-dimensional problems that illustrate the results described in the previous section.

In all cases, we use the following discrete system. Let $\Omega = (0,1)$, $\Omega_a = (0,a)$, $\Omega_b = (a,c)$, and $\Omega_c = (c,1)$, where $0 < a < c < 1$. See Figure 2. In $\Omega_c \cup \Omega_b = [a,1]$, we

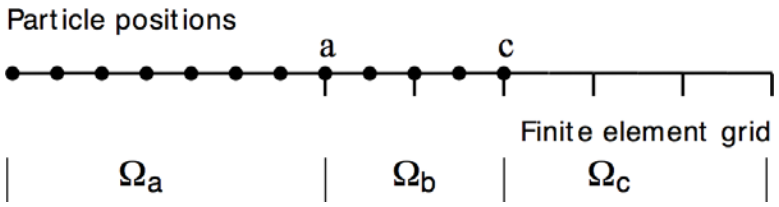

FIG. 2. *Particle positions and finite element grid for commensurate grids with* $h = 2s$.

have a uniform finite element subdivision with grid size h given by $x_j = a + (j-1)h$, $j = 1, \ldots, J$. We choose W^h to be the continuous, piecewise linear finite element space with respect to this subdivision. In $\Omega_a \cup \Omega_b = [0, c]$, we have a uniform particle lattice[23] with lattice spacing s given by $x_\alpha = (\alpha - 1)s$, $\alpha = 1, \ldots, N$. The blending functions read as

$$\theta_a(x) = \begin{cases} 1, & x \in \Omega_a, \\ 1 - \frac{x-a}{c-a}, & x \in \Omega_b, \\ 0, & x \in \Omega_c, \end{cases} \tag{5.1}$$

and $\theta_c = 1 - \theta_a$. Without loss of generality, we assume that the blending region is defined by the finite element grid; i.e., we assume that the leftmost and rightmost finite element nodes in the bridge region $\Omega_b = [a, c]$ are located at $x = a$ and $x = c$, respectively. This assumption leads to a more convenient implementation of the algorithm for problems in two- or three-dimensional spatial regions. We will consider both the cases of commensurate and noncommensurate grids, where commensurate grids are such that the finite element grid size h is an integer multiple of the lattice spacing s. Where necessary, "ghost" particles are included in Ω_c to counteract ghost forces.

In section 5.1, the displacement of a particle in the bridge region is constrained to be the same as the continuum displacement at that point; see (3.5). A unit point force is applied at the finite element node at the end point $x = 1$, and the displacement of the particle located at the end point $x = 0$ is set to zero. Using either atomistic or finite element models, the resulting solution is one of uniform strain. Thus, we want a blended model to also recover this solution.

In section 5.2, we consider the effects of two different kinds of constraints.

5.1. Nonlocal atomic force model. We consider a simple nonlocal atomic force model where every particle interacts with its two neighbors to the left and to the right as a mass-spring system. Here we choose the nearest-neighbor elastic modulus $K_1 = 50$ and the second-nearest-neighbor elastic modulus to be $K_2 = 25$. We then choose $K_c = K_1 + 2K_2 = 100$ so that the strain energies match exactly in the case of a uniform deformation field. This choice should produce a uniform strain of 0.01. For all of the following four examples, we see that Method II fails the patch test, while Method III passes, as predicted.

Example 5.1. We have the simplest case possible: the lattice spacing s is equal to the mesh width h so that there is a finite element node at every particle position. Thus, the particle lattice and finite element grid are commensurate. We also have a particle and a finite element node located at both $x = a$ and $x = c$, the end points of the bridge region. For Figure 3, we choose $h = s = 0.05$, 16 particles plus a ghost

[23] Recall that here x denotes positions in the reference, or undeformed configuration.

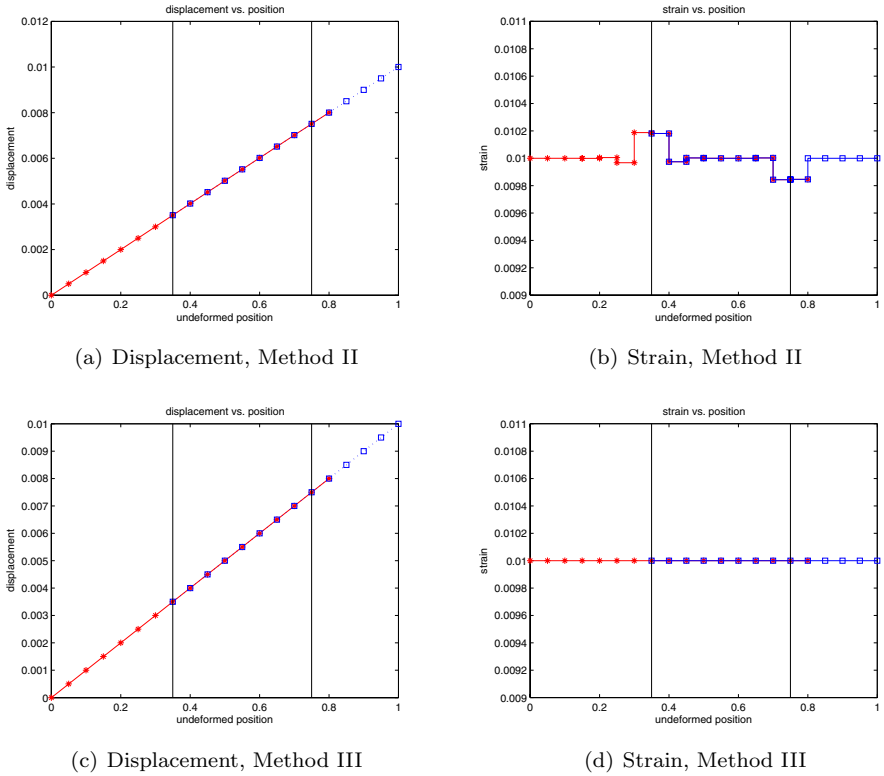

(a) Displacement, Method II

(b) Strain, Method II

(c) Displacement, Method III

(d) Strain, Method III

FIG. 3. *Displacements and strains for Example* 5.1 *at the particle positions* $*$ *and the finite element nodes* $\square$. *Vertical bars denote the bridge region.*

particle, and 14 finite element nodes so that $a = 0.35$ and $c = 0.8$. This figure shows the computed displacements and strains for Methods II and III. In this particular example, the 16th atom from the left is not located at c, and hence its associated blending weight $\theta_a(x_{16})$ is not zero. To avoid the ghost forces associated with a missing bond to the right, another atom is added to the right of node c. Its blending weight $\theta_a(x_{17})$ is zero, since the atom is contained in Ω_c, and hence we need not be concerned with its missing right bond.

Example 5.2. The setup of this example is the same as for Example 5.1, except that we now set the mesh width h to be twice the lattice spacing s. Again, the particle lattice and finite element grid are commensurate with no offset, and we have a particle and a finite element node located at both $x = a$ and $x = c$, the end points of the bridge region. We choose $s = 0.05$, 15 particles plus a ghost particle, and 8 finite element nodes so that now $a = 0.3$ and $c = 0.7$. In Figure 4, we show the computed displacements and strains.

Example 5.3. We next set $h = 1.5s$. The finite element grid and the particle lattice are no longer commensurate. We still have both a particle and a finite element node located at the points $x = a$ and $x = c$. We choose $s = 1/30$, 19 particles plus a ghost particle, and 15 finite element nodes so that $a = 0.3$ and $c = 0.6$. In Figure 5, we show the computed displacements and strains.

Example 5.4. This example is identical to Example 5.3, except that no particle is located at $x = a$, the leftmost finite element grid point, and $x = c$, the rightmost finite

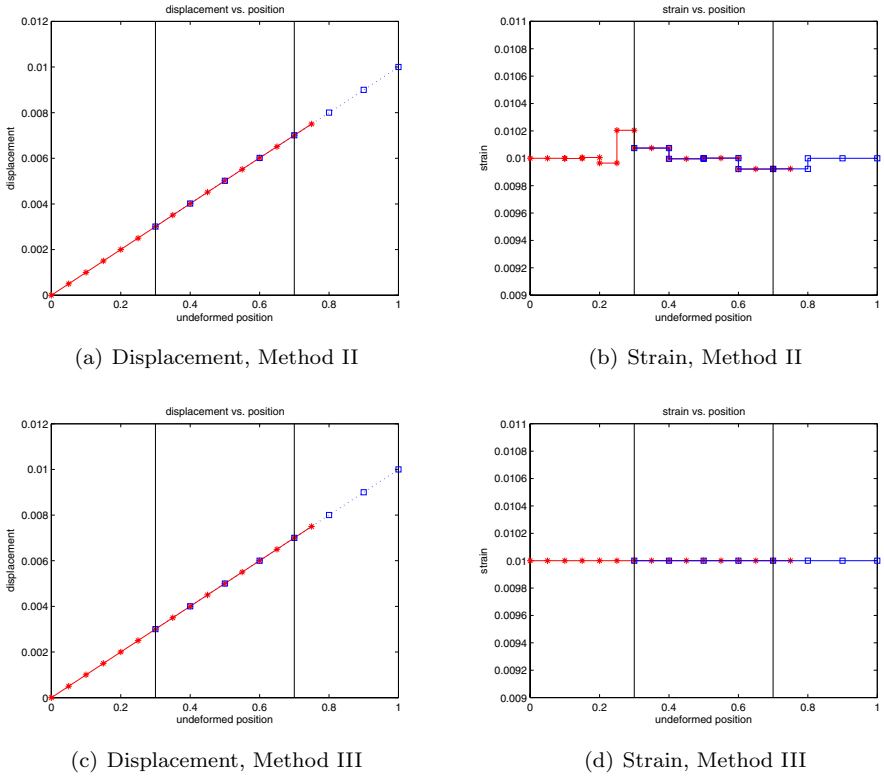

(a) Displacement, Method II

(b) Strain, Method II

(c) Displacement, Method III

(d) Strain, Method III

FIG. 4. *Displacements and strains for Example* 5.2 *at the particle positions* $*$ *and the finite element nodes* $\square$. *Vertical bars denote the bridge region.*

element grid point in the bridge region. In Figure 6, we show computed displacements and strains for a case of 20 particles plus a ghost particle, and 16 finite element nodes for Methods II and III.

5.2. Constraint operators and Lagrange multipliers. In this section, we consider two different constraint operators. The first operator is the one defined by (3.5) or (3.6), which enforces the atomistic solution to be identical to the finite element solution. We denote this choice as the *strong constraint*. The other alternative is to consider a weaker continuity of solutions where the mean value of atomistic and continuum solutions must be equal at every finite element in the blending region; i.e., we have that (3.8) holds with the subdivision $\{\Omega_{b,j}\}_{j=1}^{J}$ being the same as the finite element subdivision of Ω_b. Consequently, we refer to this choice as the *loose constraint*.

We start by analyzing Method III. Let us consider a uniform load over the whole domain. The displacement for this AtC problem is shown in Figure 7(a). Figure 7(b) compares the fully atomistic solution with the atomistic solution on the blending domain, using strong and loose constraints, for a fixed finite element mesh. The loose constraint allows the atomistic solution enough freedom to reproduce the curvature seen in the fully atomistic one, leading to better results. The strong constraint is too restrictive, forcing the atomistic solution to follow the finite element solution. It substantially reduces the accuracy within the blending region.

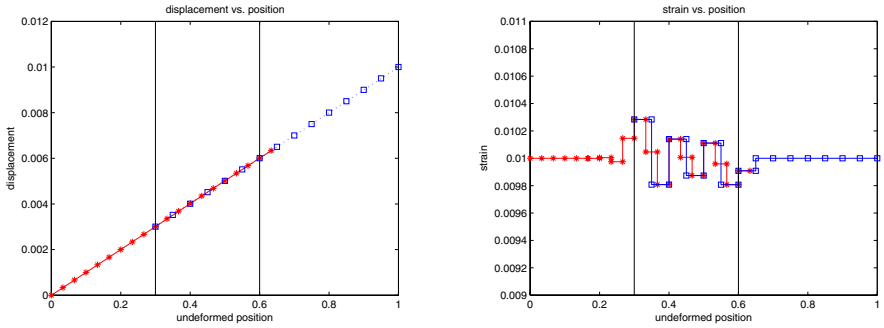

(a) Displacement, Method II (b) Strain, Method II

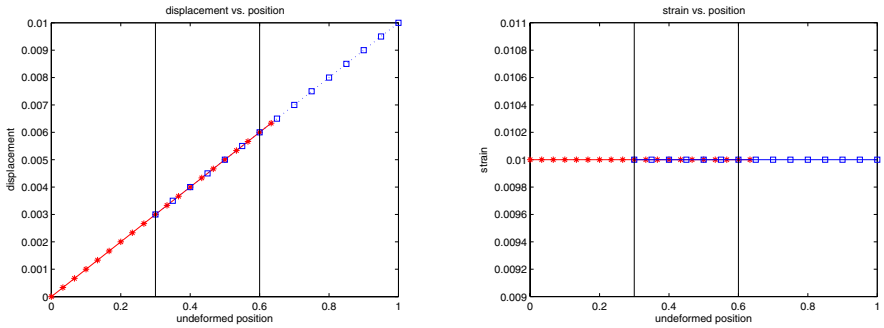

(c) Displacement, Method III (d) Strain, Method III

FIG. 5. *Displacements and strains for Example* 5.3 *at the particle positions* $*$ *and the finite element nodes* $\square$. *Vertical bars denote the bridge region.*

The strong solution is related to the Lagrange multipliers space $Q \equiv X^a$; i.e., the Lagrange multipliers are elements of the atomistic space restricted to the blending region. On the contrary, the second choice is related to a finite element space Q_h composed of elementwise constant functions. In this last case, we approximate the constraint

$$\begin{aligned} \int_{\Omega_e} \boldsymbol{\lambda}(\boldsymbol{u} - \pi_b(\boldsymbol{\psi}))\,\mathrm{d}\Omega &= \boldsymbol{\lambda} \int_{\Omega_e} (\boldsymbol{u} - \pi_b(\boldsymbol{\psi}))\,\mathrm{d}\Omega \\ &\simeq \mathrm{meas}(\Omega_e)\boldsymbol{\lambda} \sum_{\boldsymbol{x}_\alpha \in \Omega_e} (\boldsymbol{u}(\boldsymbol{x}_\alpha) - \boldsymbol{\psi}_\alpha) \end{aligned} \tag{5.2}$$

for every finite element on Ω_b. This approximation reduces the computational cost, without modifying the nature of the constraint.[24] The strong constraint is simply defined by (3.5). For numerical purposes, let us scale (3.5) with a characteristic interatomic distance.

In Figure 8, we plot the Lagrange multiplier values for the strong constraint. The atomistic lattice is kept constant, whereas the mesh size of the finite element problem is reduced, until reaching the value of the characteristic interatomic distance. We

[24] Let us remark that the interatomic distance will vary smoothly in the blending region, assuming a Cauchy–Born-type solution.

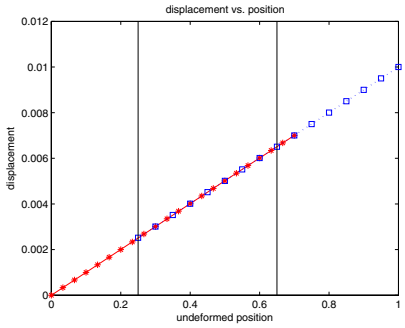

(a) Displacement, Method II

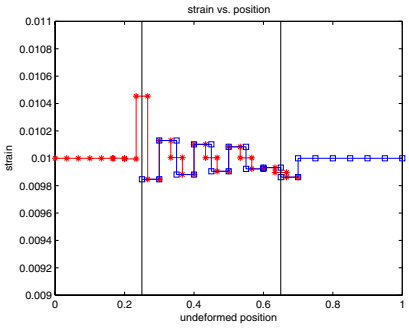

(b) Strain, Method II

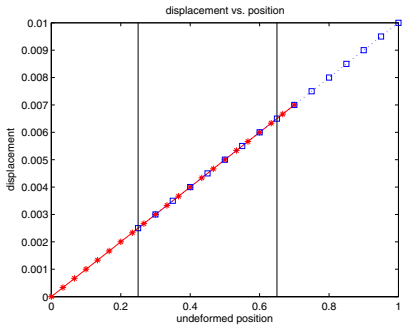

(c) Displacement, Method III

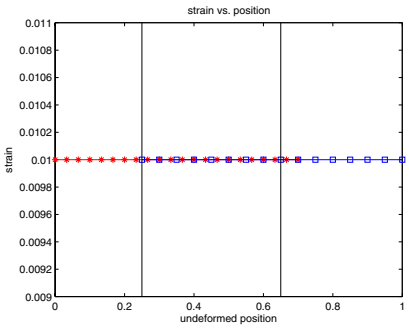

(d) Strain, Method III

FIG. 6. *Displacements and strains for Example* 5.4 *at the particle positions* $*$ *and the finite element nodes* $\square$. *Vertical bars denote the bridge region.*

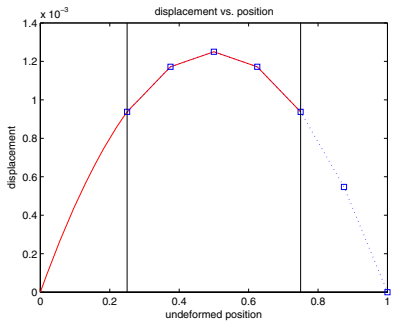

(a) AtC displacement for a distributed load

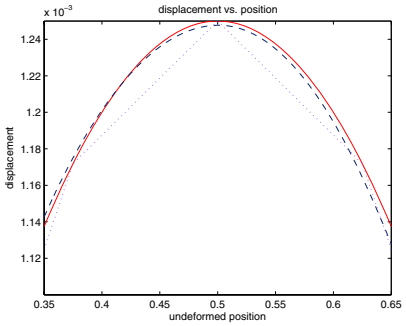

(b) Comparison of the fully atomistic solution (solid line) with loose constraint (dashed line) and strong constraint (dotted line)

FIG. 7. *Application of a uniform load over the problem domain. The AtC solution for Method* III *is shown in* (a) *and strong and loose constraints compared in* (b).

can see the nonsmooth nature of the Lagrange multiplier. In fact, this result is in agreement with the stability discussion. The Lagrange multiplier is bounded in a weak norm (a negative norm). Whereas the H^1 norm blows up, the L^2 Euclidean

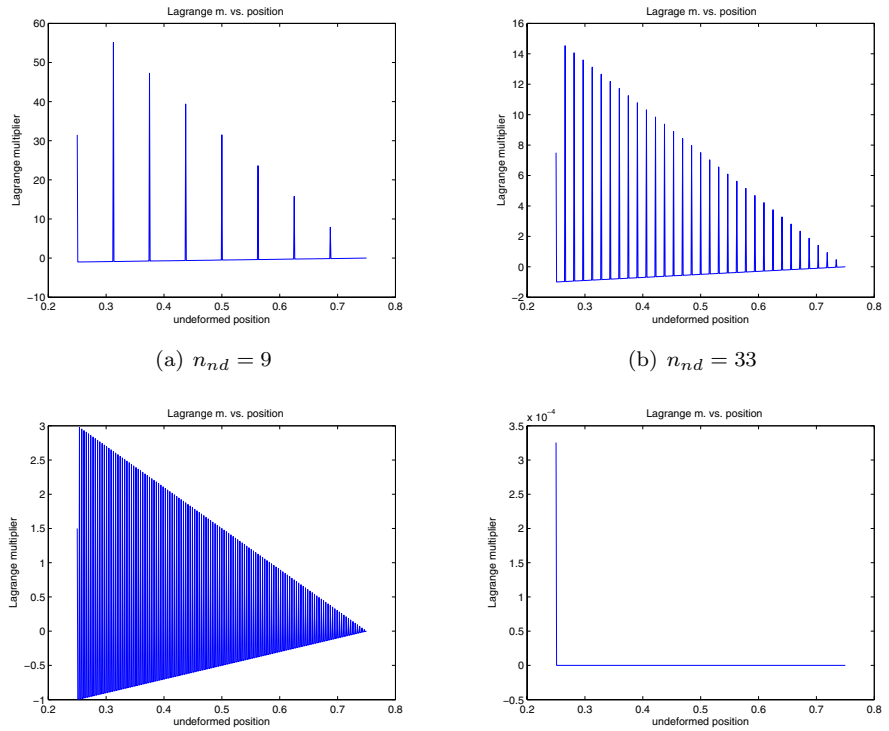

(a) $n_{nd} = 9$ (b) $n_{nd} = 33$

(c) $n_{nd} = 129$ (d) $n_{nd} = 513$

FIG. 8. *Lagrange multipliers for strong constraint and Method* III. *There are* 513 *atoms and* n_{nd} *finite element nodes on* Ω_b.

norm tends to a constant value. This result also shows that the atomistic problem on the blending region is overconstrained. We can also see that the magnitude of the peaks in Figure 8 clearly diminishes as the mesh is refined.

Figure 9 shows the same test for the loose constraint. One important aspect is the convergence of the Lagrange multiplier. In this case, the maximum values are almost constant, and the fully oscillatory behavior shown, for instance, in Figure 8(b) is not present. Again, the L^2 norm of the Lagrange multiplier does not blow up.[25]

When using a mass-spring system as the atomistic model with the appropriate stiffness when the mesh size is equal to the characteristic interatomic distance, the atomistic and finite element problems lead to the same discrete equations for the inner atoms/nodes on the blending region. At these nodes, the AtC solution is also the solution of the blended atomistic and finite element systems alone. Thus, the Lagrange multiplier must be different from zero only on the extremes of the blending region. That is, the Lagrange multipliers can be understood as point forces (on these extremes) such that the two problems lead to the same result on the blending region. See [12] for a similar discussion for continuum-to-continuum coupling.

The same numerical experiments have been carried out for Method II. In Figure 10, we show the Lagrange multipliers for strong coupling. The Lagrange multiplier plots for loose coupling are collected in Figure 11. Again, the strong constraint leads

[25] In fact, it goes to zero.

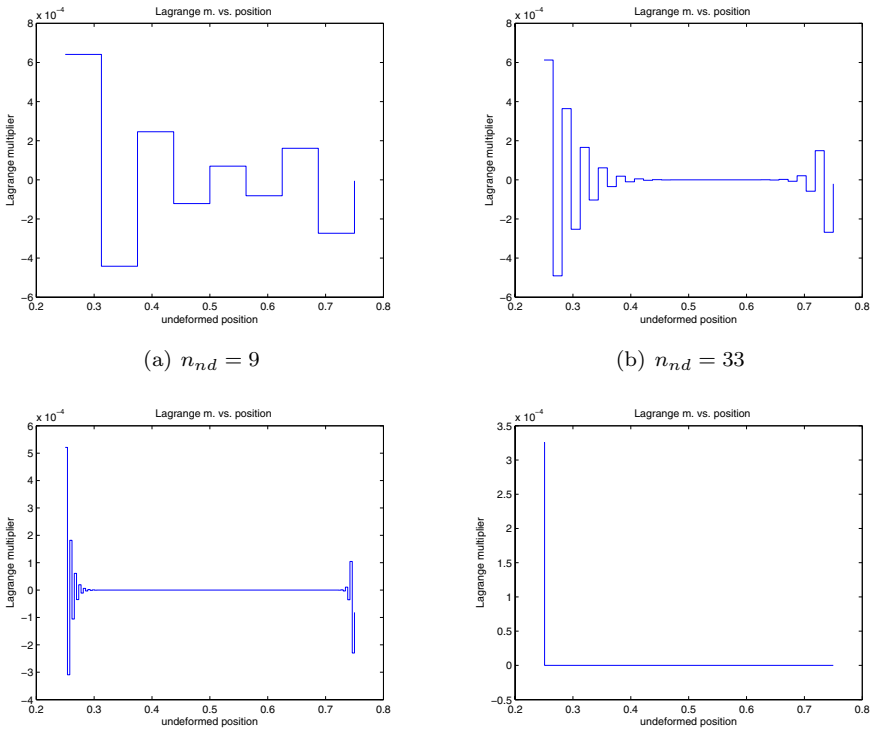

(a) $n_{nd} = 9$ (b) $n_{nd} = 33$

(c) $n_{nd} = 129$ (d) $n_{nd} = 513$

FIG. 9. *Lagrange multipliers for loose constraint and Method* III. *There are* 513 *atoms and* n_{nd} *finite element nodes on* Ω_b.

to highly oscillatory results. Better results are obtained using the looser constraint. The main difference with respect to the results for Method III is the converged solution when the mesh size is equal to the characteristic interatomic distance. The Lagrange multipliers do not vanish in the interior of Ω_b because neither the atomistic nor the continuum problems alone are satisfied by the AtC solution at atoms/nodes in the interior of Ω_b. Furthermore, the maximum Lagrange multiplier value increases when the mesh size is reduced.

Even though the characteristic interatomic distance is a physical parameter, it is interesting to analyze the asymptotic behavior of the loose constraint when this parameter tends to zero. In Figure 12, we see that the L^2 norm does not blow up when the interatomic distance tends to zero.

These computational experiments suggest a preference for the use of loose constraints for AtC blended coupling. Furthermore, in contradiction to [12], the Lagrange multiplier does not exhibit any instability for L^2 coupling. This is of particular interest, because the use of stronger H^1 constraints is too expensive in AtC coupling.

Finally, let us remark that, in order to mitigate ghost forces, we introduce ghost particles in the continuum region.[26] This saturates the bonds of the particles in $\Omega_b \cup \Omega_c$. These ghost particles are simply implemented as slaves of the continuum displacement in Ω_c (using the strong constraint (3.5)), without invoking the atomistic

[26]In fact, only particles in the cut-off radius of particles in $\Omega_b \cup \Omega_c$ are needed.

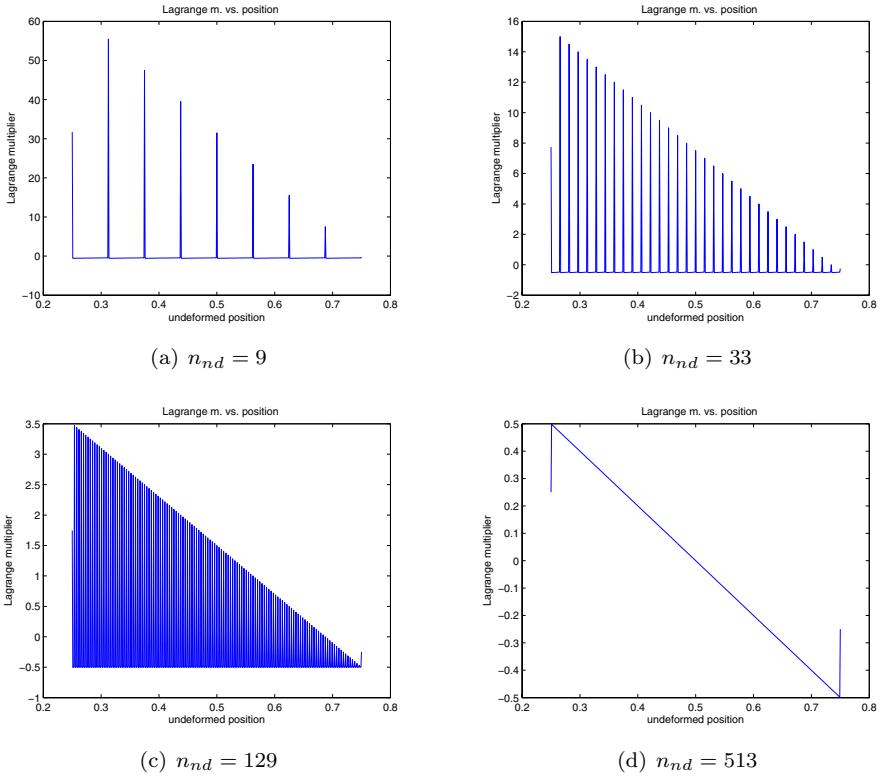

(a) $n_{nd} = 9$ (b) $n_{nd} = 33$

(c) $n_{nd} = 129$ (d) $n_{nd} = 513$

FIG. 10. *Lagrange multipliers for strong constraint and Method* II. *There are* 513 *atoms and* n_{nd} *finite element nodes on* Ω_b.

problem. This is the difference between ghost particles and particles in the blending region (for the strong constraint). In the first case the displacement is determined only by the continuum model whereas in the second one by a blending between atomistic and continuum problems.

6. Conclusions. In this article, we have introduced a novel mathematical framework for describing AtC blended coupling techniques and outlined the two main ingredients for defining these methods. The first ingredient is the choice of blended model on the blending region. In particular, we have shown four classes of AtC blending methods. The second ingredient is the constraints that must be enforced to provide continuity to the coupled solution.

The choice of how to enforce these constraints does not modify the final result but has important implications for the implementation of these methods. We have considered two different choices: classical Lagrange multipliers, and restricted AtC spaces whose elements explicitly satisfy the constraints.

This framework has been useful for the analysis of the consistency of the different methods. We have introduced a notion of consistency for AtC coupling methods, formalized the notion of a patch test problem, the origin of ghost forces, and addressed whether Newton's third law is satisfied.

Finally, we have checked the theoretical consistency results through numerical experimentation. We have studied the stability of the Lagrange multipliers and have

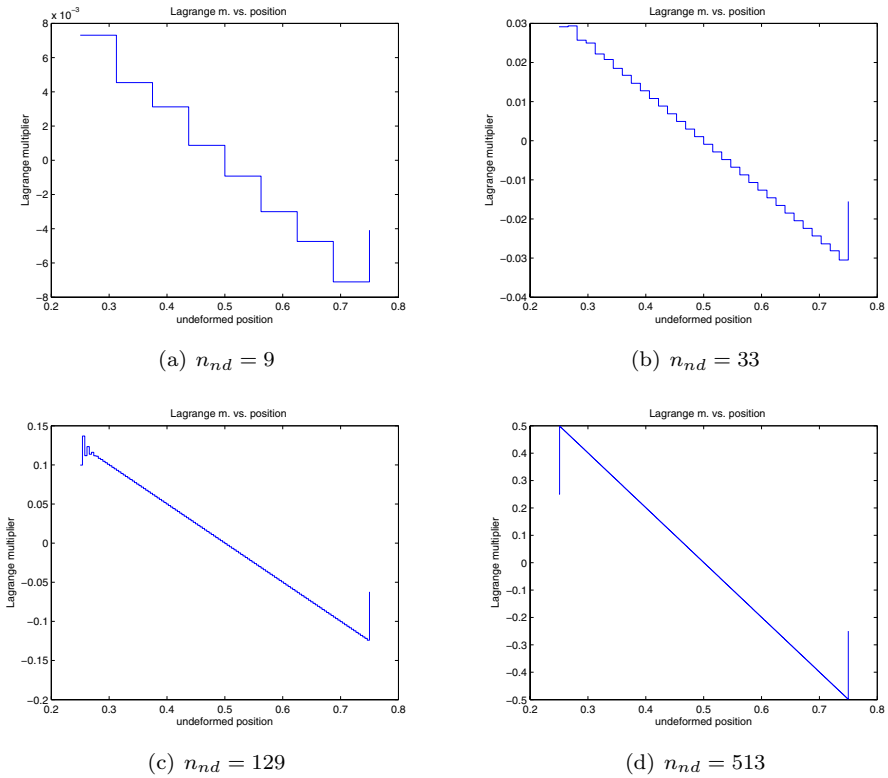

(a) $n_{nd} = 9$ (b) $n_{nd} = 33$

(c) $n_{nd} = 129$ (d) $n_{nd} = 513$

FIG. 11. *Lagrange multipliers for loose constraint and Method* II. *There are* 513 *atoms and* n_{nd} *finite element nodes on* Ω_b.

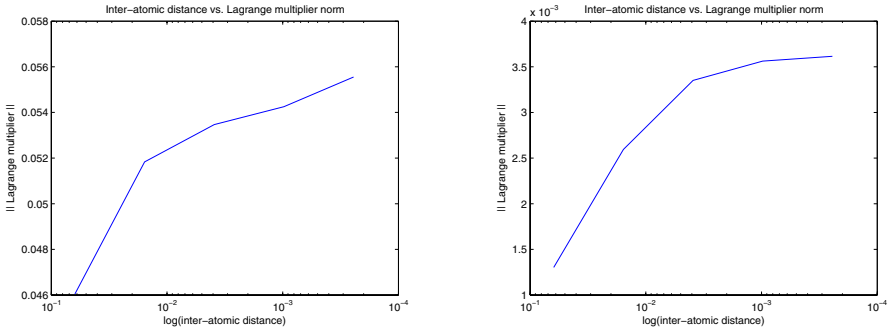

(a) Method II (b) Method III

FIG. 12. L^2 *norm of the Lagrange multiplier vs. characteristic interatomic distance.*

discussed a good choice for the space of these Lagrange multipliers. We considered two different cases, a space that overconstrains the atomistic solution and a looser constraint that leads to better numerical results.

These results have allowed us to identify that the blended model introduced in [3] is not consistent and that the method suggested in [1] is more accurate. Finally, we

have suggested a new method that is consistent and passes any patch test problem (in the sense introduced in the article).

REFERENCES

[1] S. Badia, P. Bochev, J. Fish, M. Gunzburger, R. Lehoucq, M. Nuggehally, and M. Parks, *A force-based blending model for atomistic-to-continuum coupling*, Int. J. Mult. Comp. Eng., 5 (2007), pp. 387–406.

[2] P. T. Bauman, H. Ben Dhia, N. Elkhodja, J. T. Oden, and S. Prudhomme, *On the application of the Arlequin method to the coupling of particle and continuum models*, Comput. Mech., to appear.

[3] T. Belytschko and S. P. Xiao, *Coupling methods for continuum model with molecular model*, Int. J. Mult. Comp. Eng., 1 (2003), pp. 115–126.

[4] T. Belytschko and S. P. Xiao, *A bridging domain method for coupling continua with molecular dynamics*, Comput. Methods Appl. Mech. Engrg., 193 (2004), pp. 1645–1669.

[5] X. Blanc, C. Le Bris, and F. Legoll, *Analysis of prototypical multiscale method coupling atomistic and continuum mechanics*, M2AN Math. Model. Numer. Anal., 39 (2005), pp. 797–826.

[6] M. Born and K. Huang, *Dynamical Theory of Crystal Lattices*, Clarendon Press, Oxford, UK, 1954.

[7] F. Brezzi and M. Fortin, *Mixed and Hybrid Finite Element Methods*, Springer-Verlag, New York, 1991.

[8] W. A. Curtin and R. E. Miller, *Atomistic/continuum coupling methods in multi-scale materials modeling*, Modell. Simul. Mater. Sci. Eng., 11 (2003), pp. R33–R68.

[9] H. Ben Dhia and G. Rateau, *The Arlequin method as a flexible engineering design tool*, Internat. J. Numer. Methods Engrg., 62 (2005), pp. 1442–1462.

[10] W. E and P. Ming, *Cauchy–Born rule and the stability of crystalline solids: Static problems*, Arch. Ration. Mech. Anal., 183 (2007), pp. 241–297.

[11] J. Fish, M. A. Nuggehally, M. S. Shephard, C. R. Picu, S. Badia, M. L. Parks, and M. Gunzburger, *Concurrent AtC coupling based on a blend of the continuum stress and the atomistic force*, Comput. Methods Appl. Mech. Engrg., 196 (2007), pp. 4548–4560.

[12] P.-A. Guidault and T. Belytschko, *On the L^2 and H^1 couplings for an overlapping domain method using Lagrange multipliers*, Internat. J. Numer. Methods Engrg., 70 (2007), pp. 322–350.

[13] J. Knap and M. Ortiz, *An analysis of the quasicontinuum method*, J. Mech. Phys. Solids, 49 (2001), pp. 1899–1923.

[14] P. Lin, *Theoretical and numerical analysis for the quasi-continuum approximation of a material particle model*, Math. Comp., 72 (2003), pp. 657–675.

[15] P. Lin, *Convergence analysis of a quasi-continuum approximation for a two-dimensional material without defects*, SIAM J. Numer. Anal., 45 (2007), pp. 313–332.

[16] R. Miller and E. Tadmor, *The quasicontinuum method: Overview, applications and current directions*, J. Comput. Aided Mater. Des., 9 (2002), pp. 203–239.

[17] J. T. Oden, S. Prudhomme, A. Romkes, and P. T. Bauman, *Multiscale modeling of physical phenomena: Adaptive control of models*, SIAM J. Sci. Comput., 28 (2006), pp. 2359–2389.

[18] E. B. Tadmor, M. Ortiz, and R. Phillips, *Quasicontinuum analysis of defects in solids*, Philos. Mag. A, 73 (1996), pp. 1529–1563.